Electronic Supplementary Information (ESI)

Deep eutectic solvents – based green absorbents for effective volatile organochlorine compounds removal from biogas

Patrycja Makoś-Chełstowska [1]*, Edyta Słupek [1], Jacek Gębicki [1]

[1] Department of Process Engineering and Chemical Technology, Faculty of Chemistry, Gdansk University of Technology, G. Narutowicza St. 11/12, 80–233 Gdańsk, Poland; edyta.slupek@pg.edu.pl (E.S.); jacek.gebicki@pg.edu.pl (J.G.)

*Correspondence: patrycja.makos@pg.edu.pl; Tel.: +48-508-997-100

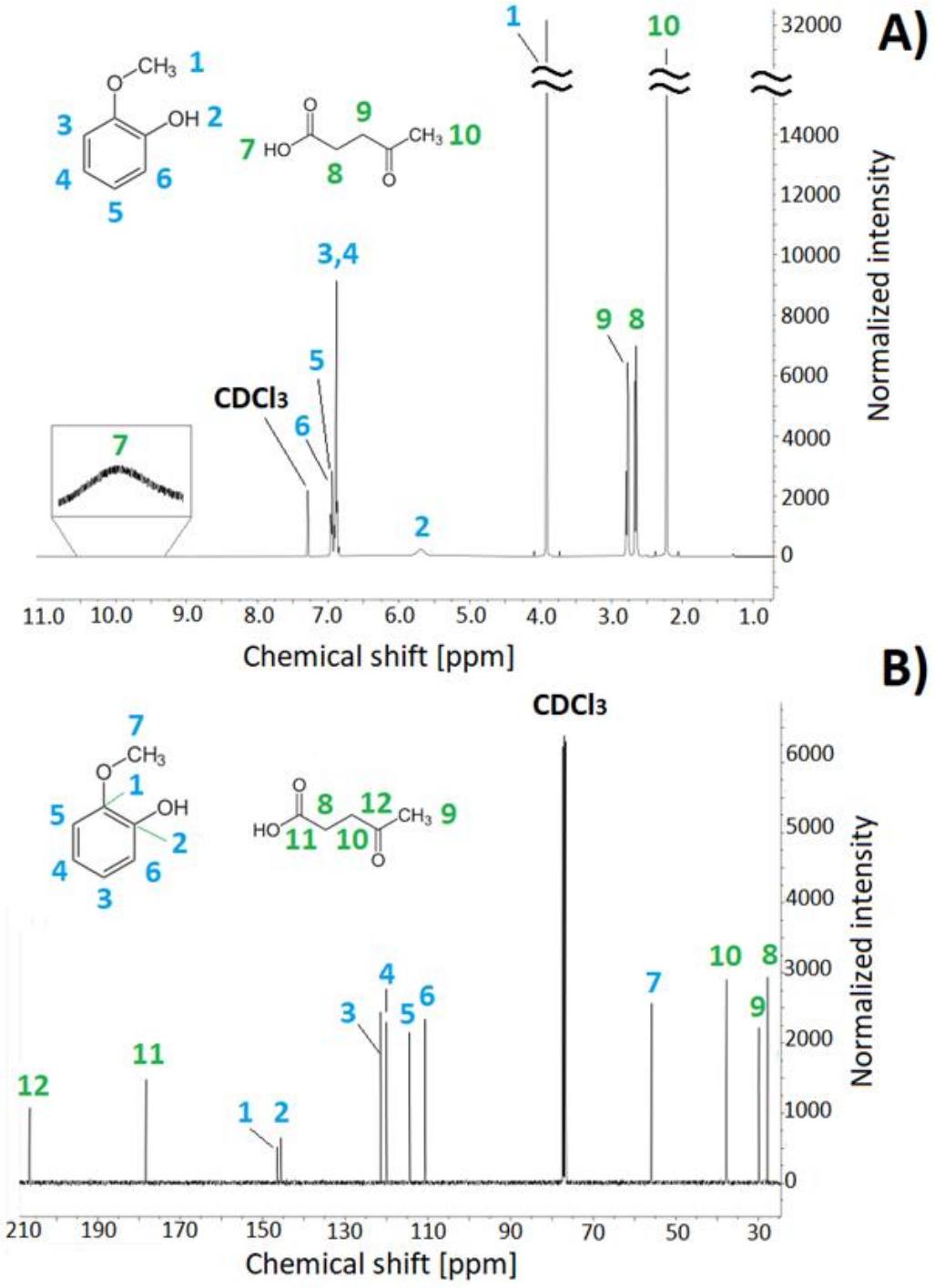

Figure S1 A) ^{1}H NMR spectra of Gu:Lev (1:1), B) ^{13}C NMR spectra of Gu:Lev (1:1).

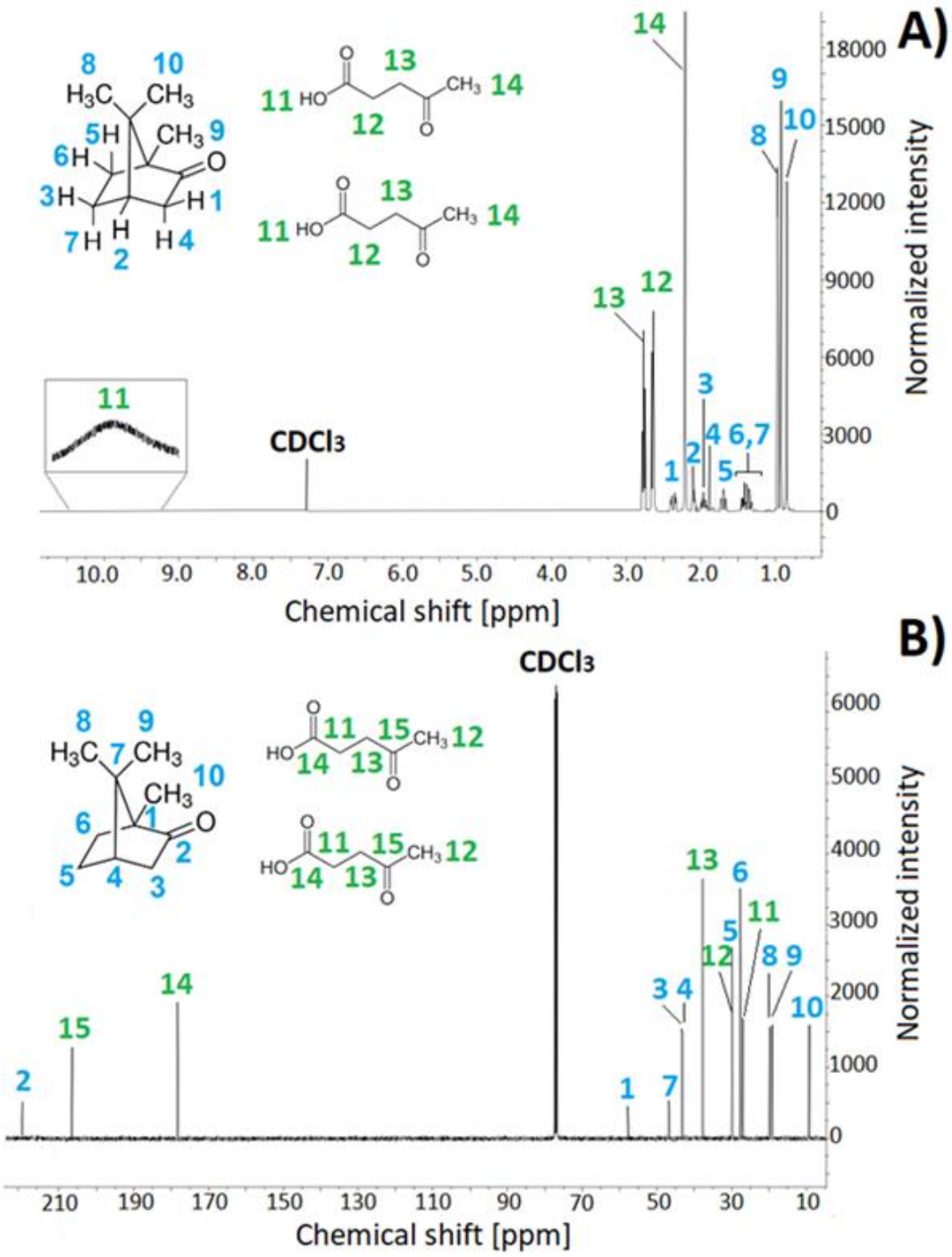

Figure S2 A) ^{1}H NMR spectra of C:Lev (1:2), B) ^{13}C NMR spectra of C:Lev (1:2).

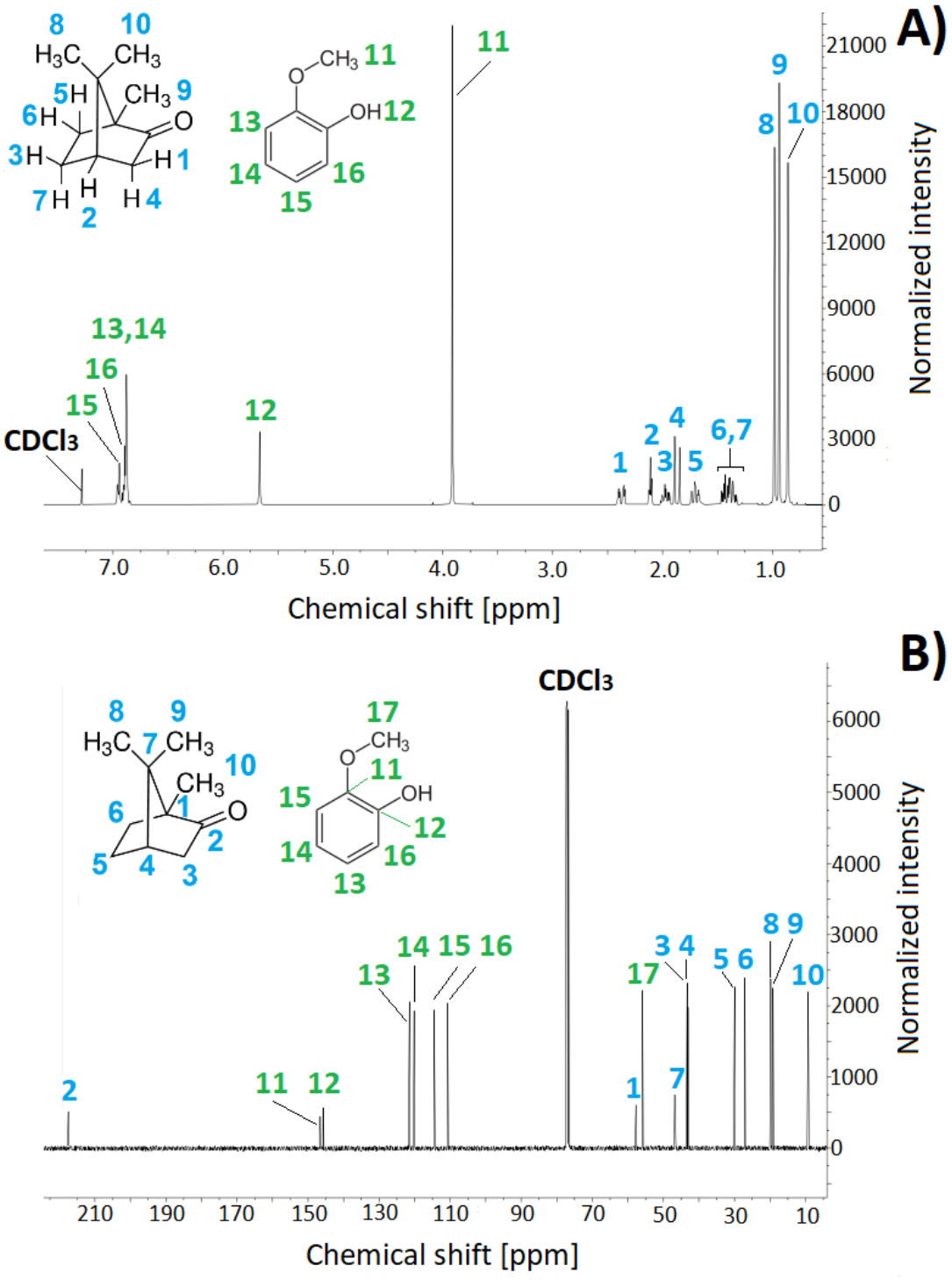

Figure S3 A) ^{1}H NMR spectra of C:Gu (1:1), B) ^{13}C NMR spectra of C:Gu (1:1).

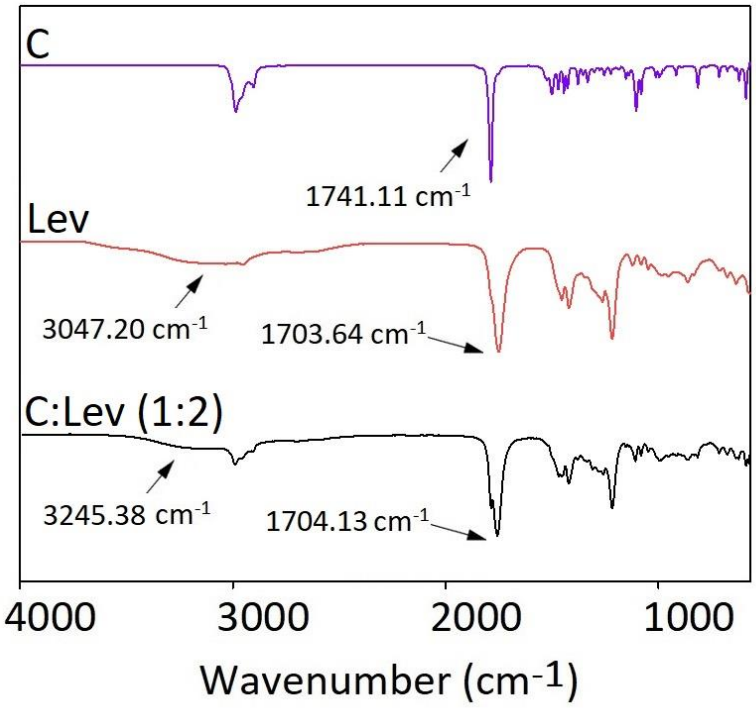

Figure S4 FT-IR spectrum for pure C, Lev, and C:Lev (1:2).

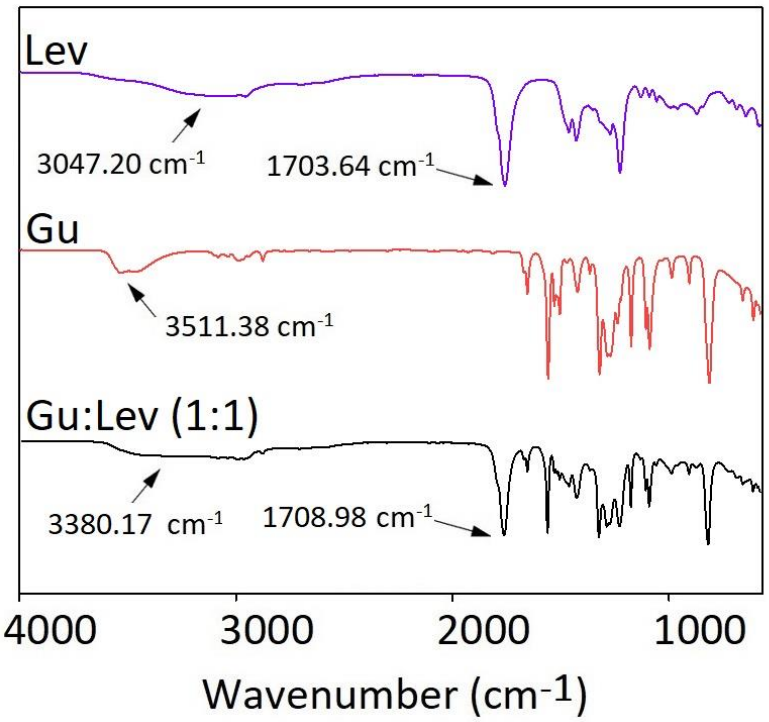

Figure S5 FT-IR spectrum for pure Lev, Gu, and Gu:Lev (1:1).

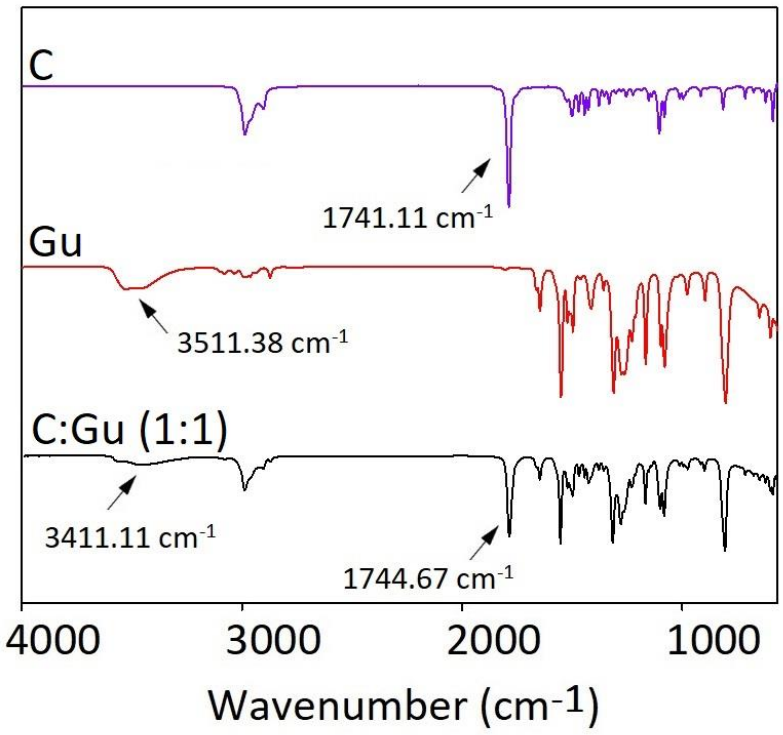

Figure S6 FT-IR spectrum for pure C, Gu, and C:Gu (1:1).

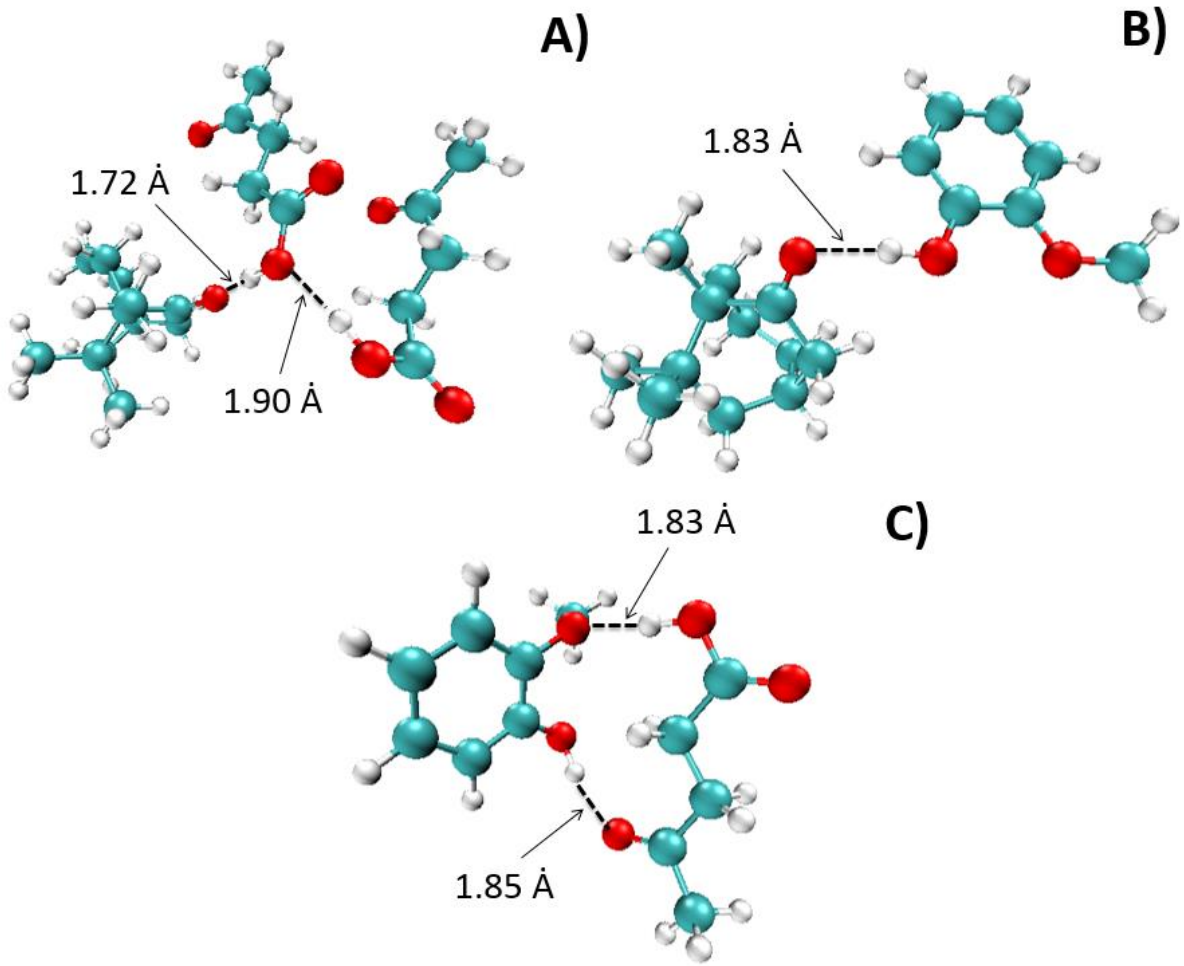

Figure S7 The structures of DESs after geometric optimization: A) C:Lev (1:2); B) C:Gu (1:1); C) Gu:Lev (1:1).

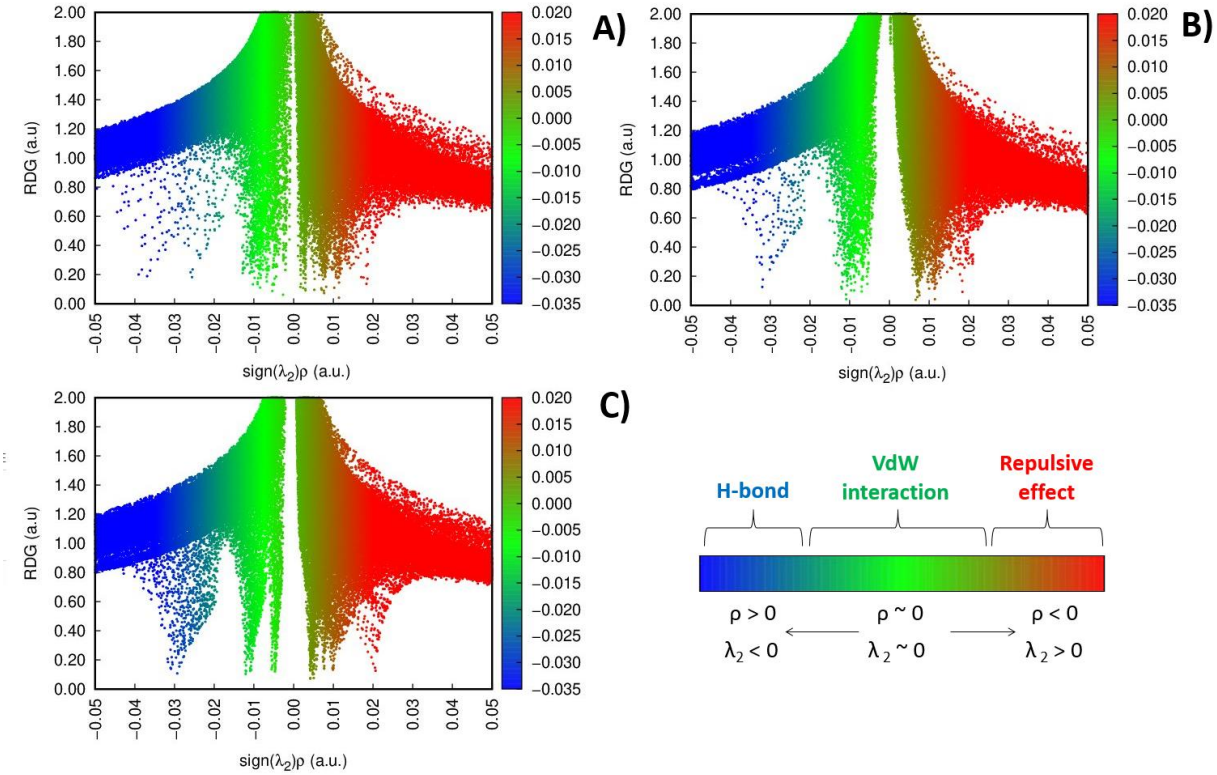

Figure S8 2D plots of RDG versus the electron density multiplied by the sign of the second Hessian eigenvalue for: A) C:Lev (1:2); B) C:Gu (1:1); C) Gu:Lev (1:1). The red area represents repulsive effects; blue area - H-bonding; green area - van der Waals interactions.

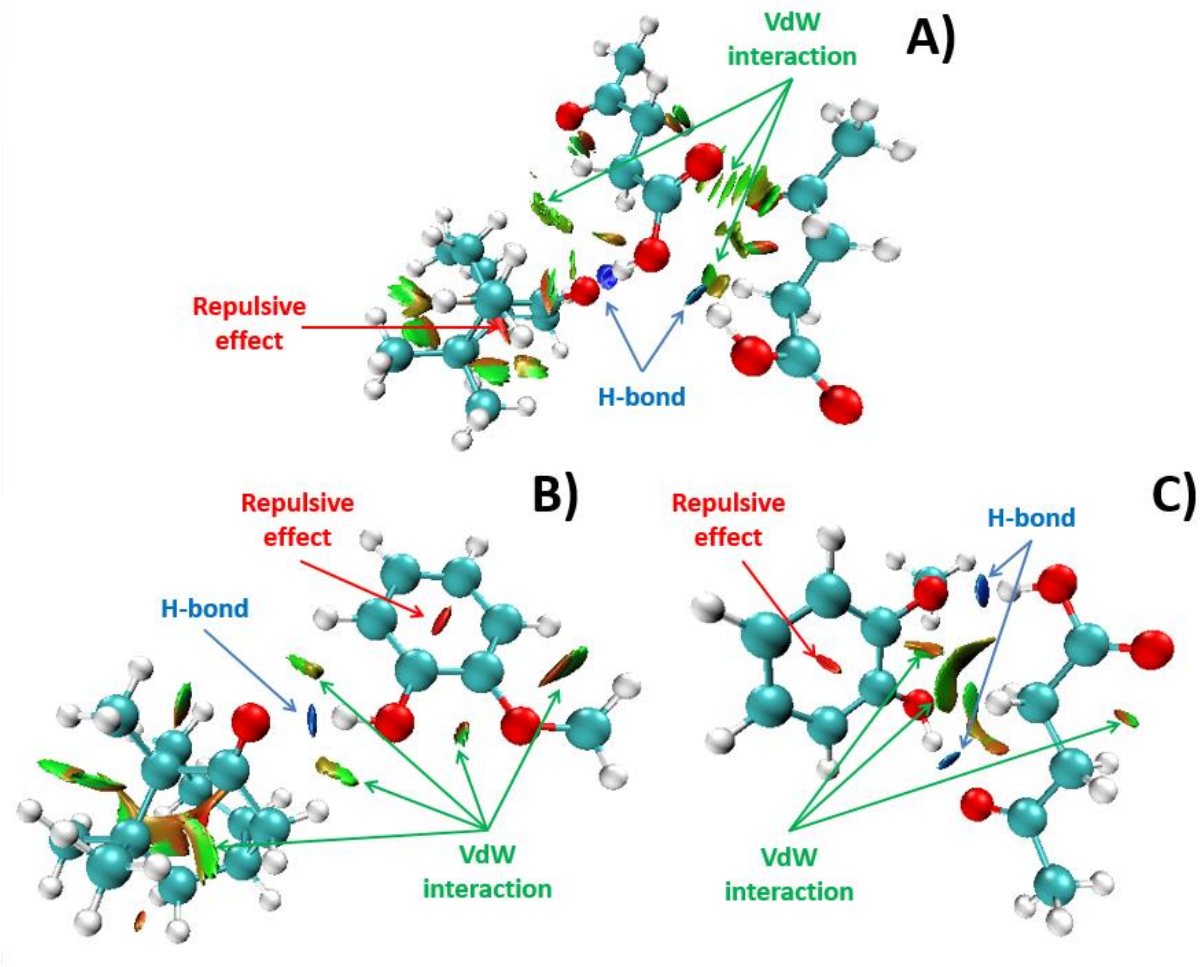

Figure S9 Reduced density gradient (RDG) isosurfaces (s=0.5 a.u.) of studied DESs: A) C:Lev (1:2); B) C:Gu (1:1); C) Gu:Lev (1:1). The red area represents repulsive effects; blue area - H-bonding; green area - van der Waals interactions.

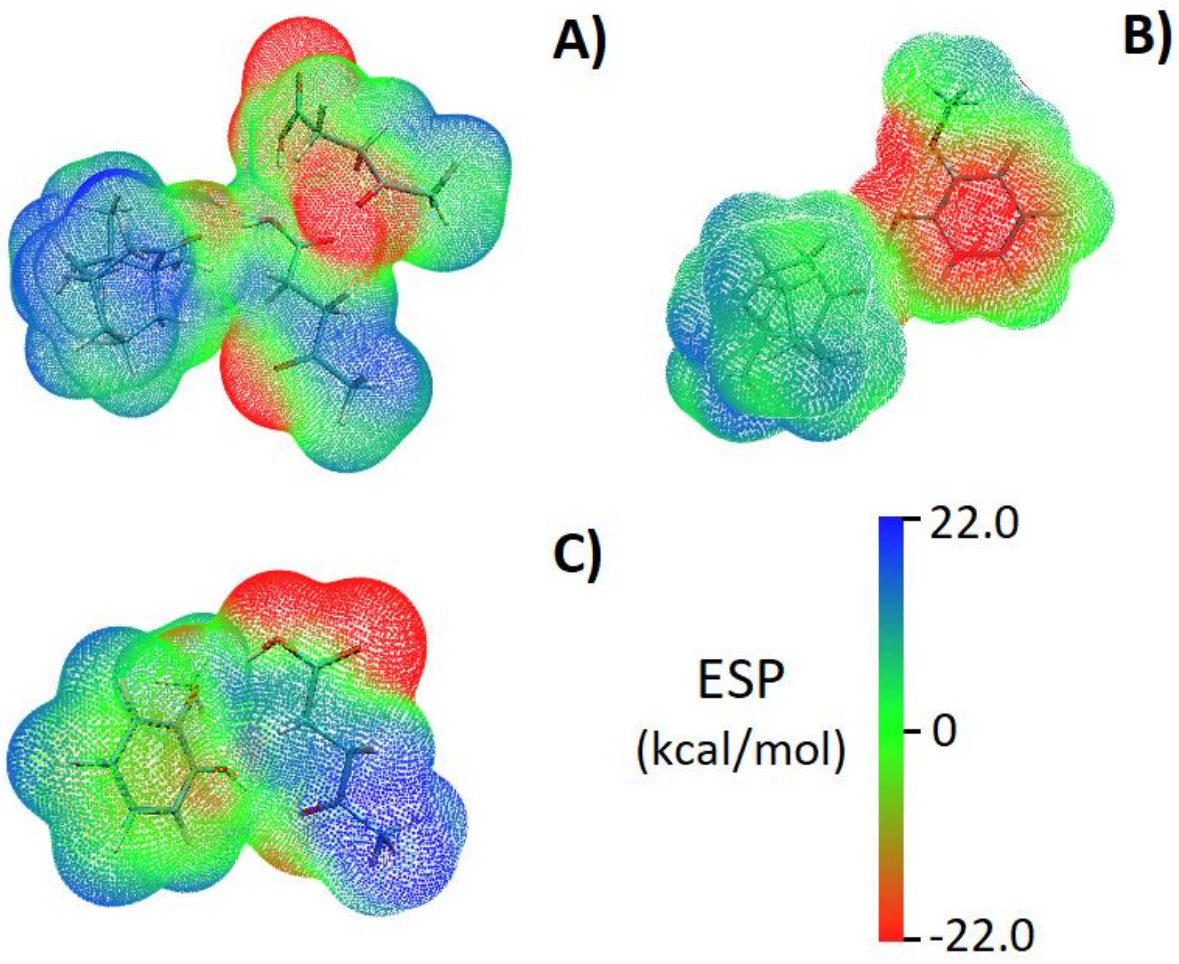

Figure S10 Elecrostatic potential (ESP) mapped on electron total density with an isovalue 0.001 for: A) C:Lev (1:2); B) C:Gu (1:1); C) Gu:Lev (1:1). Blue area are positively charged; red regions are negatively charged; green are neutrally charged.

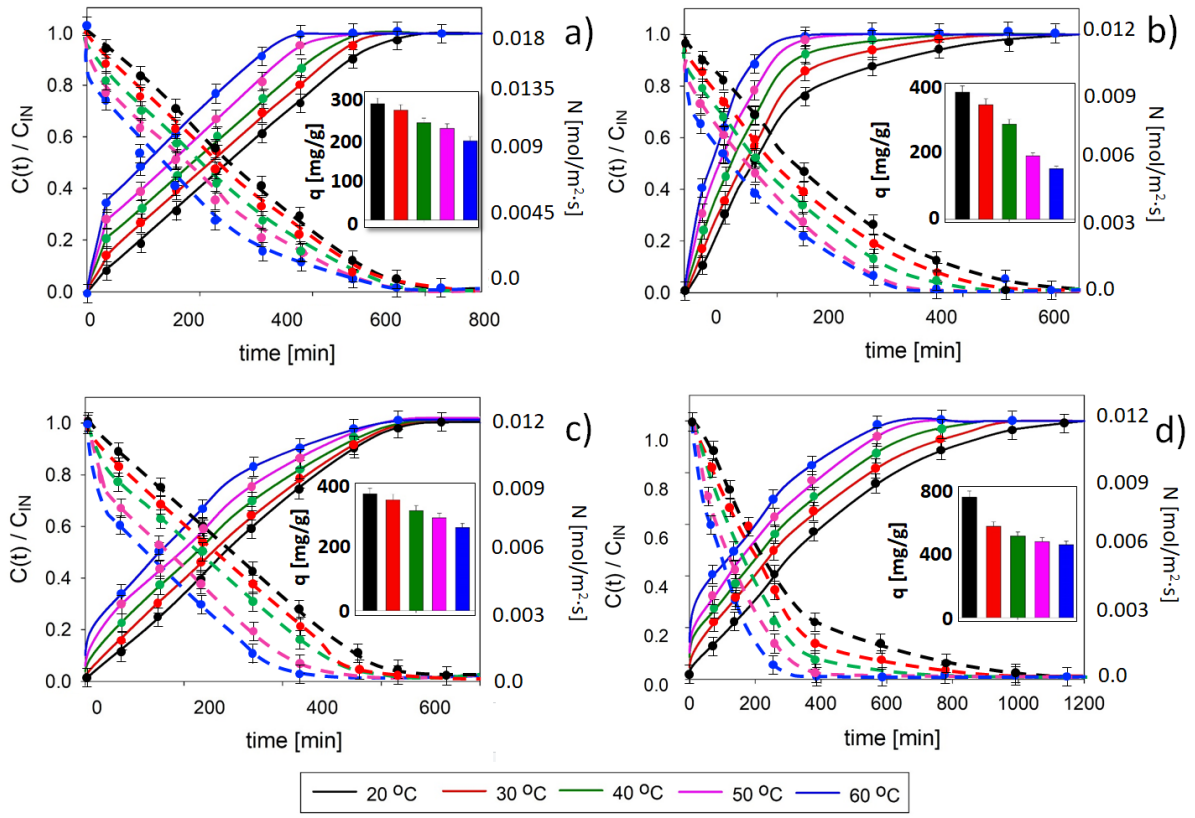

Figure S11 Experimental breakthrough curves of a) CF; b) TCM; c) TCE; d) TCEtOH at different temperatures for Syr:Lev (1:1) (inlet VOX concentration 0.5 mg/cm^3; gas flow 50 mL/min; matrix gas N_2;).

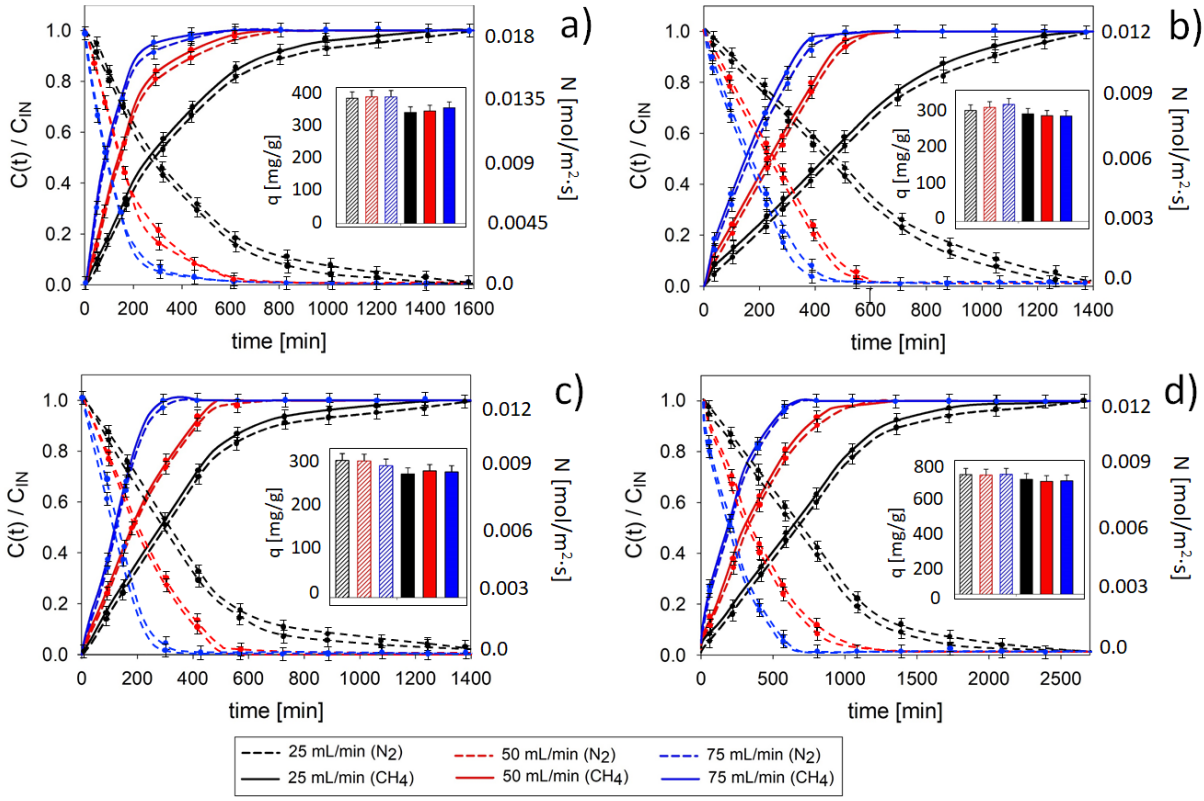

Figure S12 Experimental breakthrough curves of a) CF; b) TCM; c) TCE; d) TCEtOH at different gas flow rate for Syr:Lev (1:1) (inlet VOX concentration 0.5 mg/cm^3; temperature 20°C).

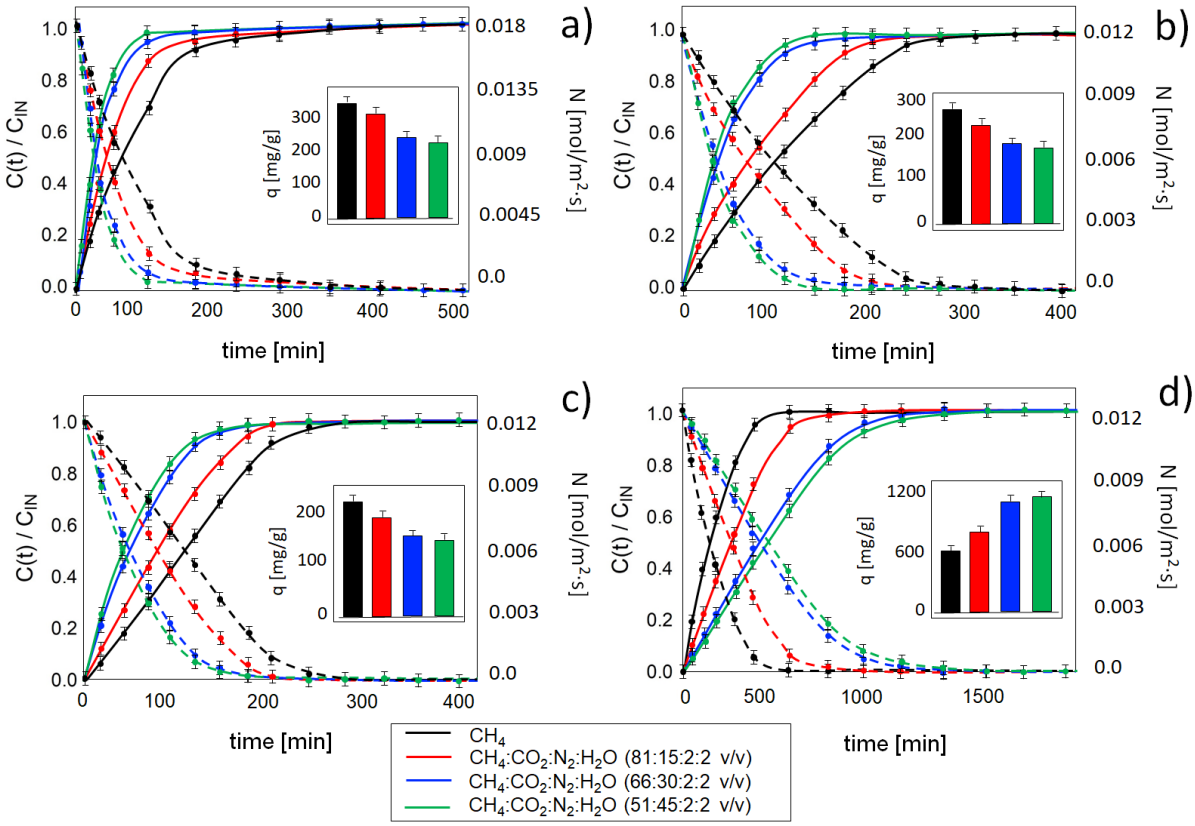

Figure S13 Experimental breakthrough curves of a) CF; b) TCM; c) TCE; d) TCEtOH at different gas matrix (inlet VOX concentration 0.5 mg/cm^3; gas flow 50 mL/min; temperature 20°C).

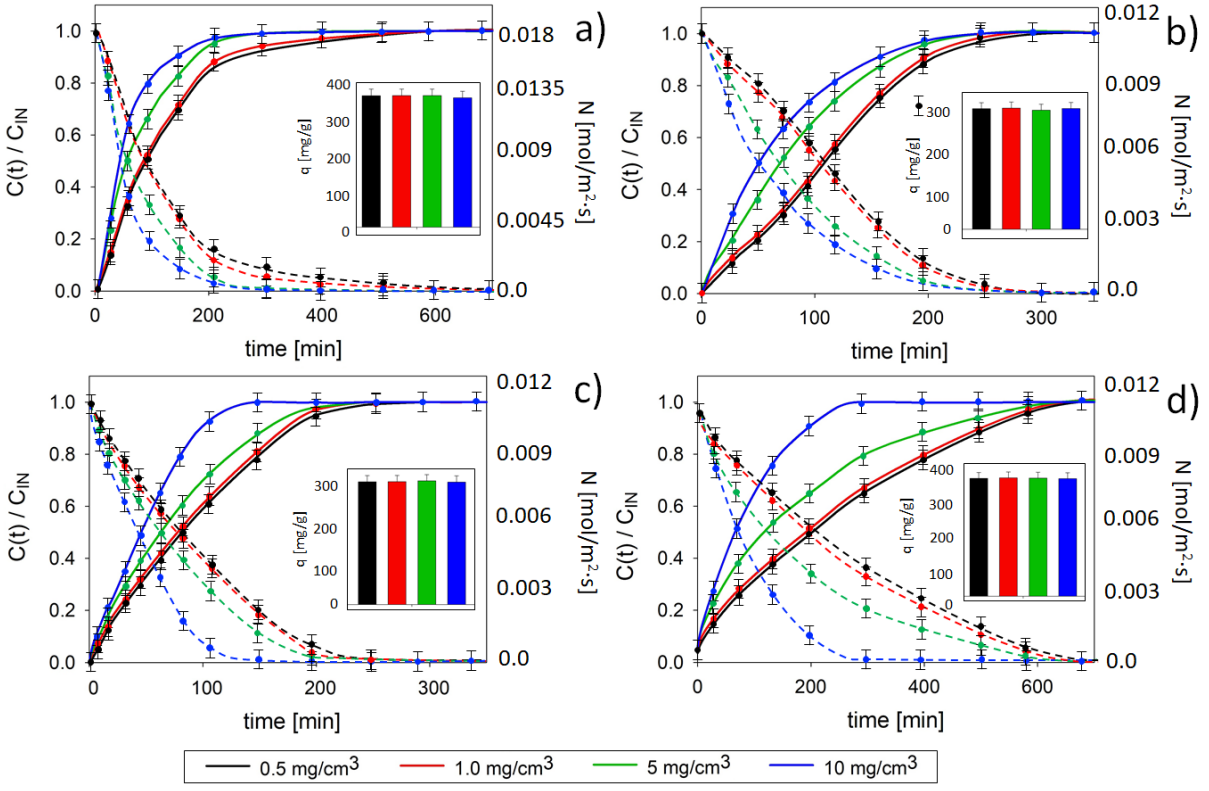

Figure S14 Experimental breakthrough curves of a) CF; b) TCM; c) TCE; d) TCEtOH at different initial concentration for Syr:Lev (1:1) (gas flow 70 mL/min; matrix gas N_2; temperature 20°C).

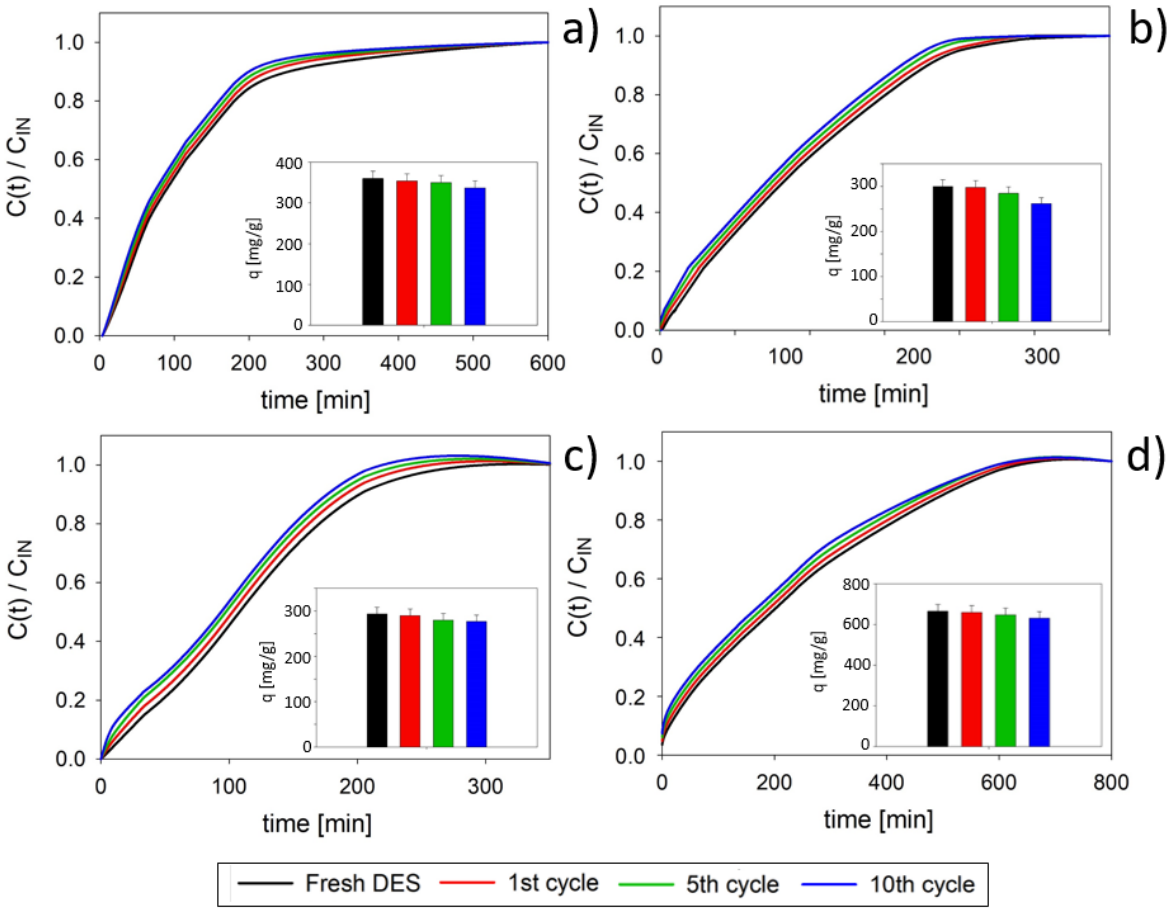

Figure S15 Experimental breakthrough curves of a) CF; b) TCM; c) TCE; d) TCEtOH after absorption/desorption cycles of Syr:Lev (1:1) (gas flow 70 mL/min; matrix gas N_2; temperature 20°C).

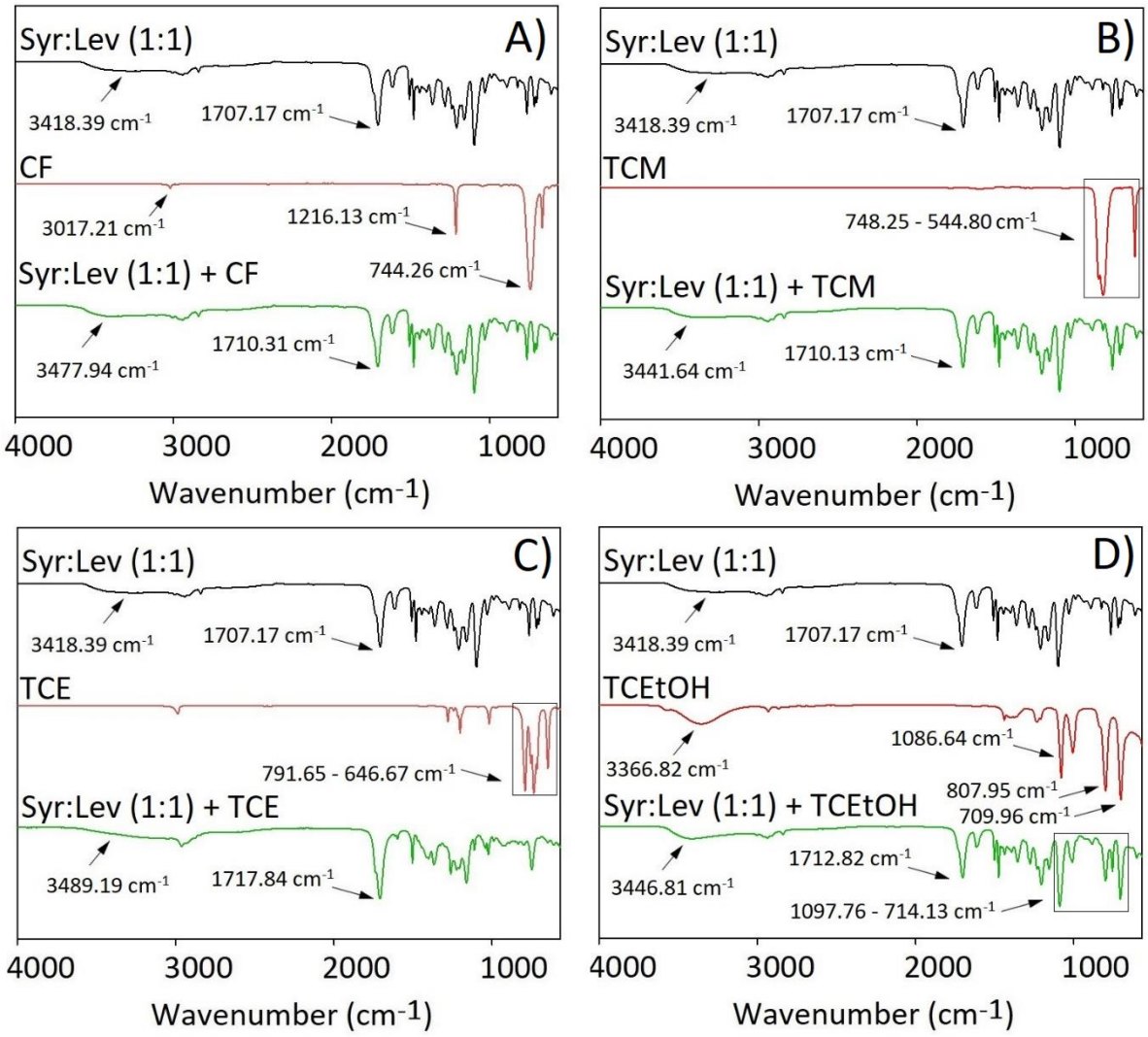

Figure S16 FT-IR spectra of pure Syr:Lev (1:1), pure VOXs, and Syr:Lev (1:1) – VOX complexes: A) Syr:Lev (1:1) – CF; B) Syr:Lev (1:1) - TCM; C) Syr:Lev (1:1) – TCE; D) Syr:Lev (1:1) - TCEtOH.

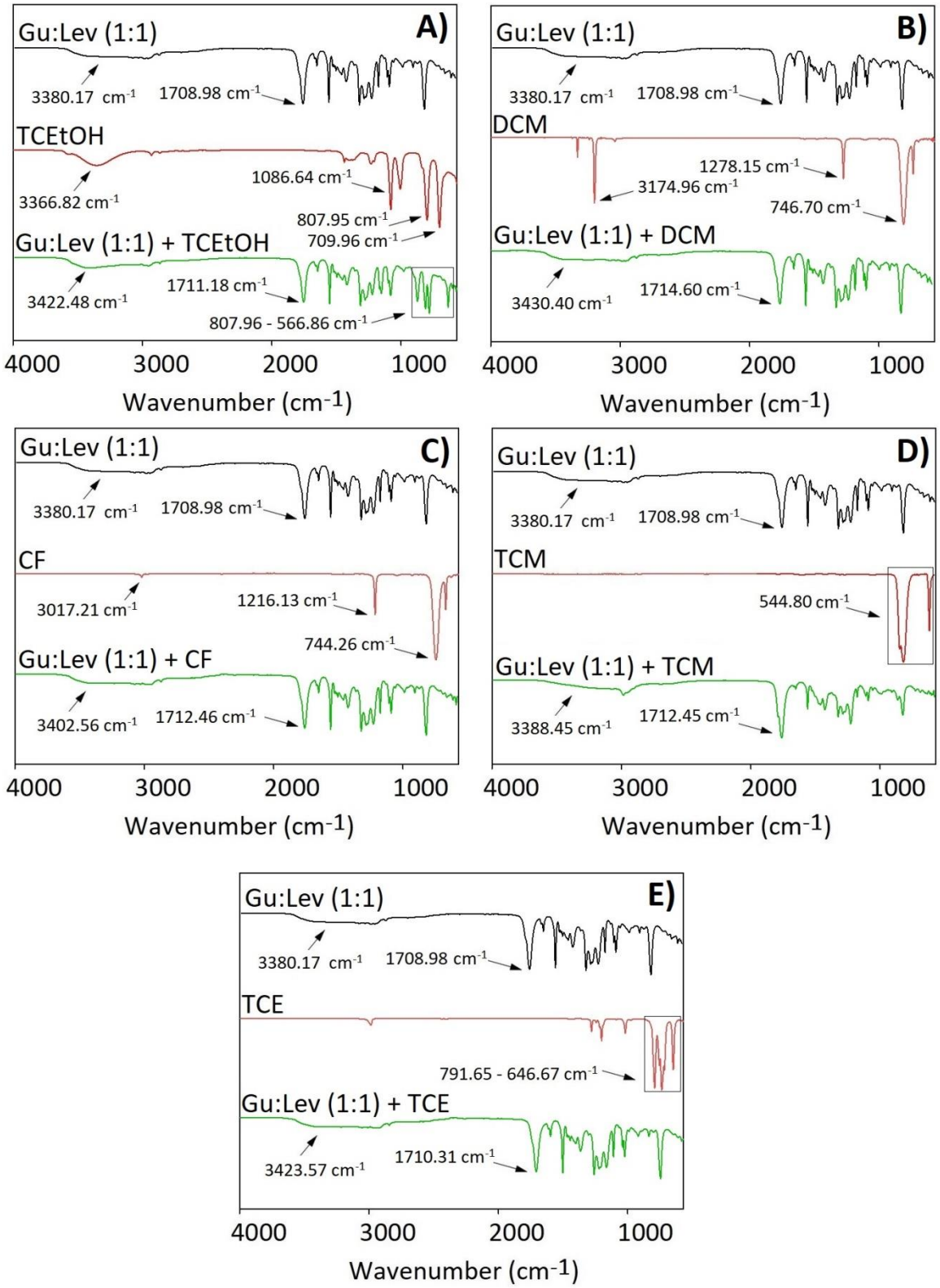

Figure S17 FT-IR spectra of pure Gu:Lev (1:1), pure VOXs, and Gu:Lev (1:1) – VOX complexes: A) Gu:Lev (1:1) - TCEtOH; B) Gu:Lev (1:1) - DCM; C) Gu:Lev (1:1) - CF; D) Gu:Lev (1:1) - TCM; E) Gu:Lev (1:1) – TCE.

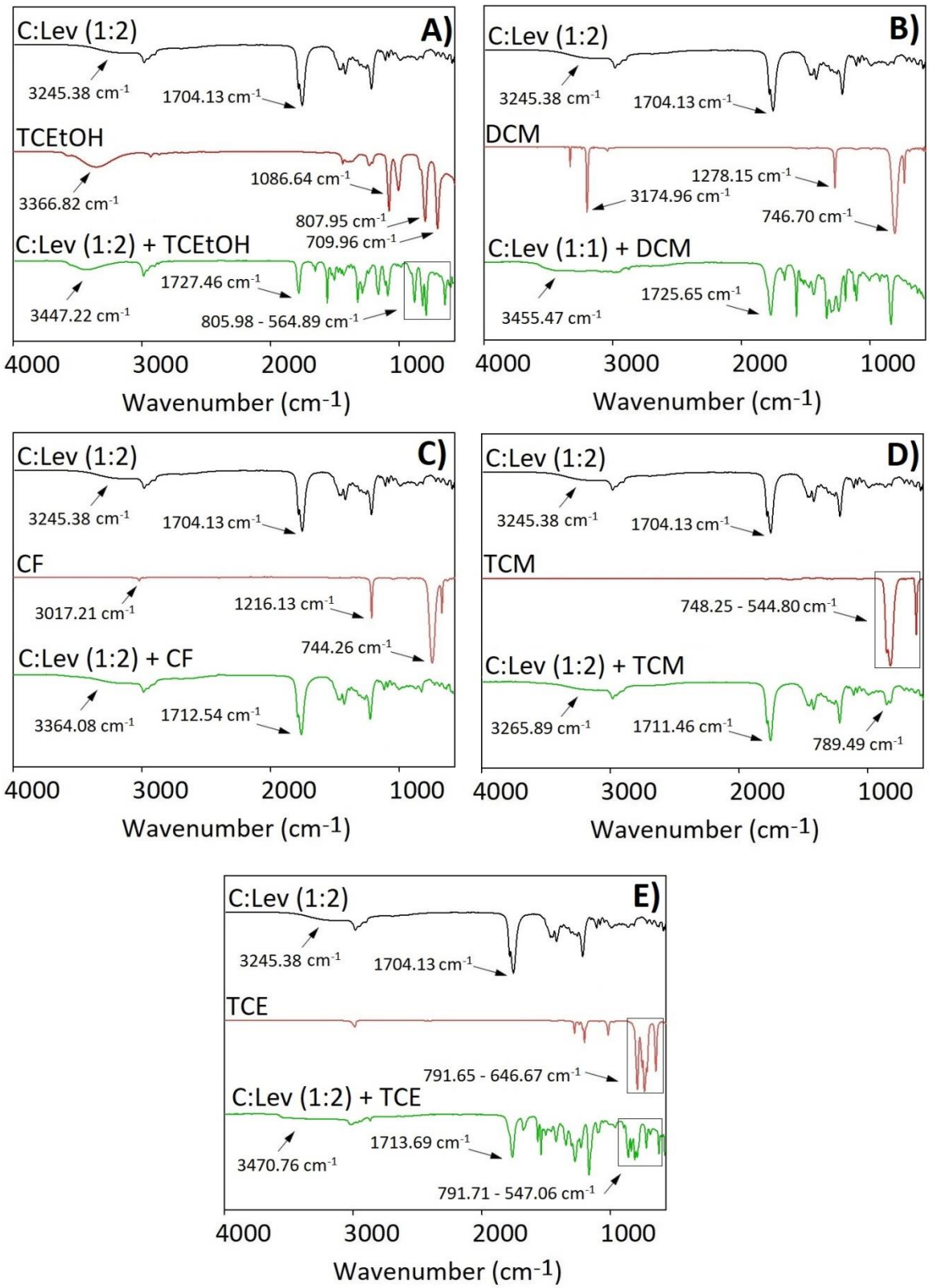

Figure S18 FT-IR spectra of pure C:Lev (1:2), pure VOXs, and C:Lev (1:2) – VOX complexes: A) C:Lev (1:2) - TCEtOH; B) C:Lev (1:2) - DCM; C) C:Lev (1:2) - CF; D) C:Lev (1:2) - TCM; E) C:Lev (1:2) – TCE.

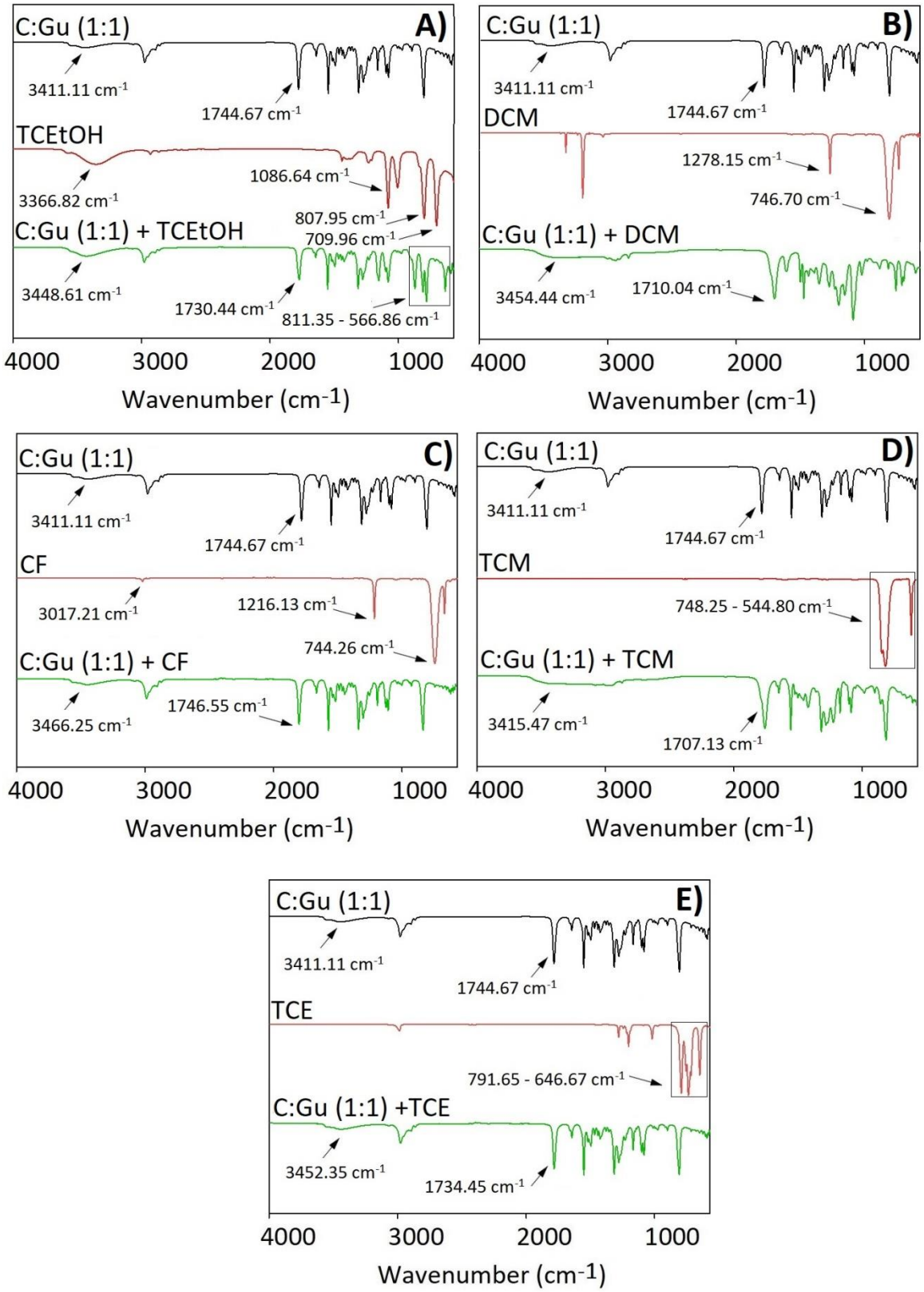

Figure S19 FT-IR spectra of pure C:Gu (1:1), pure VOXs, and C:Gu (1:1) – VOX complexes: A) C:Gu (1:1) - TCEtOH; B) C:Gu (1:1) - DCM; C) C:Gu (1:1) - CF; D) C:Gu (1:1) - TCM; E) C:Gu (1:1) – TCE.

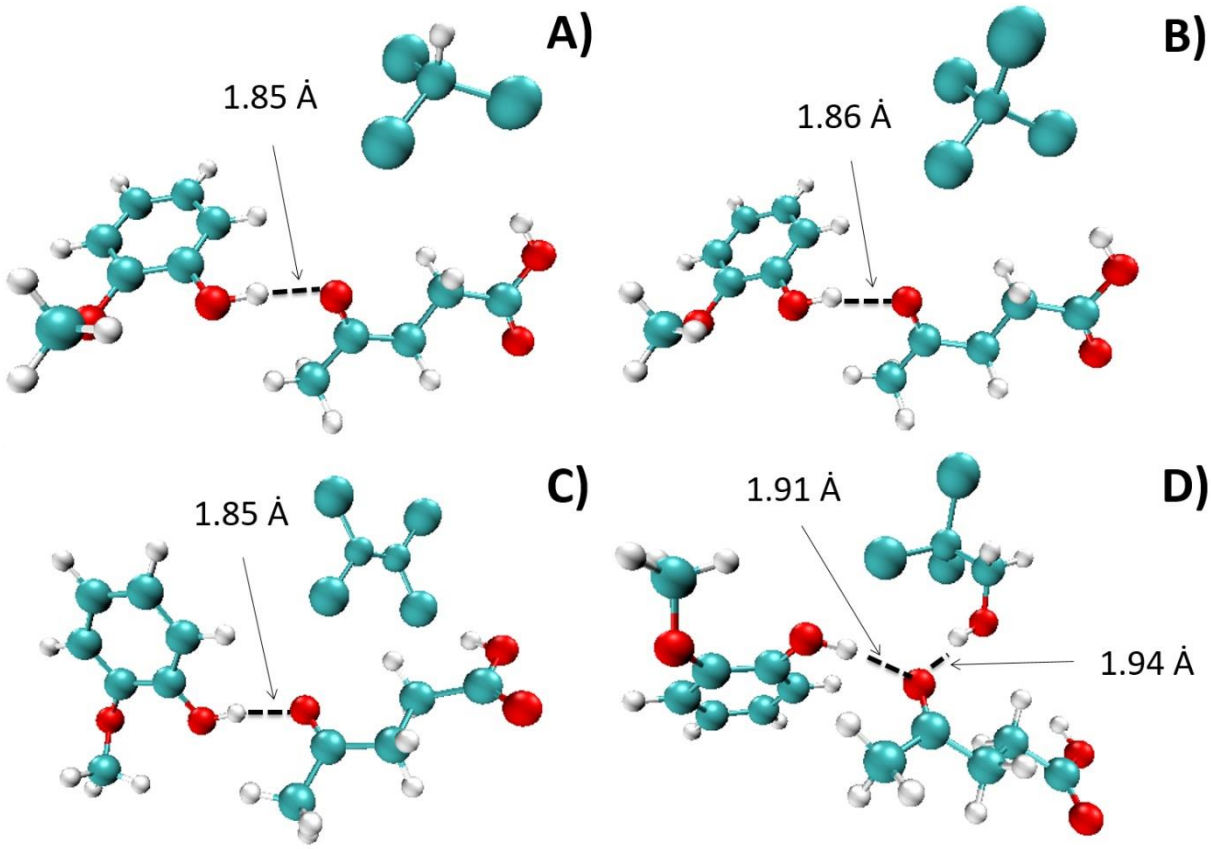

Figure S20 The structures of Syr:Lev (1:1) – VOX complexes after geometric optimization: a) A) Syr:Lev (1:1) – CF; B) Syr:Lev (1:1) – TCM; C) Syr:Lev (1:1) – TCE; D) Syr:Lev (1:1) – TCEtOH.

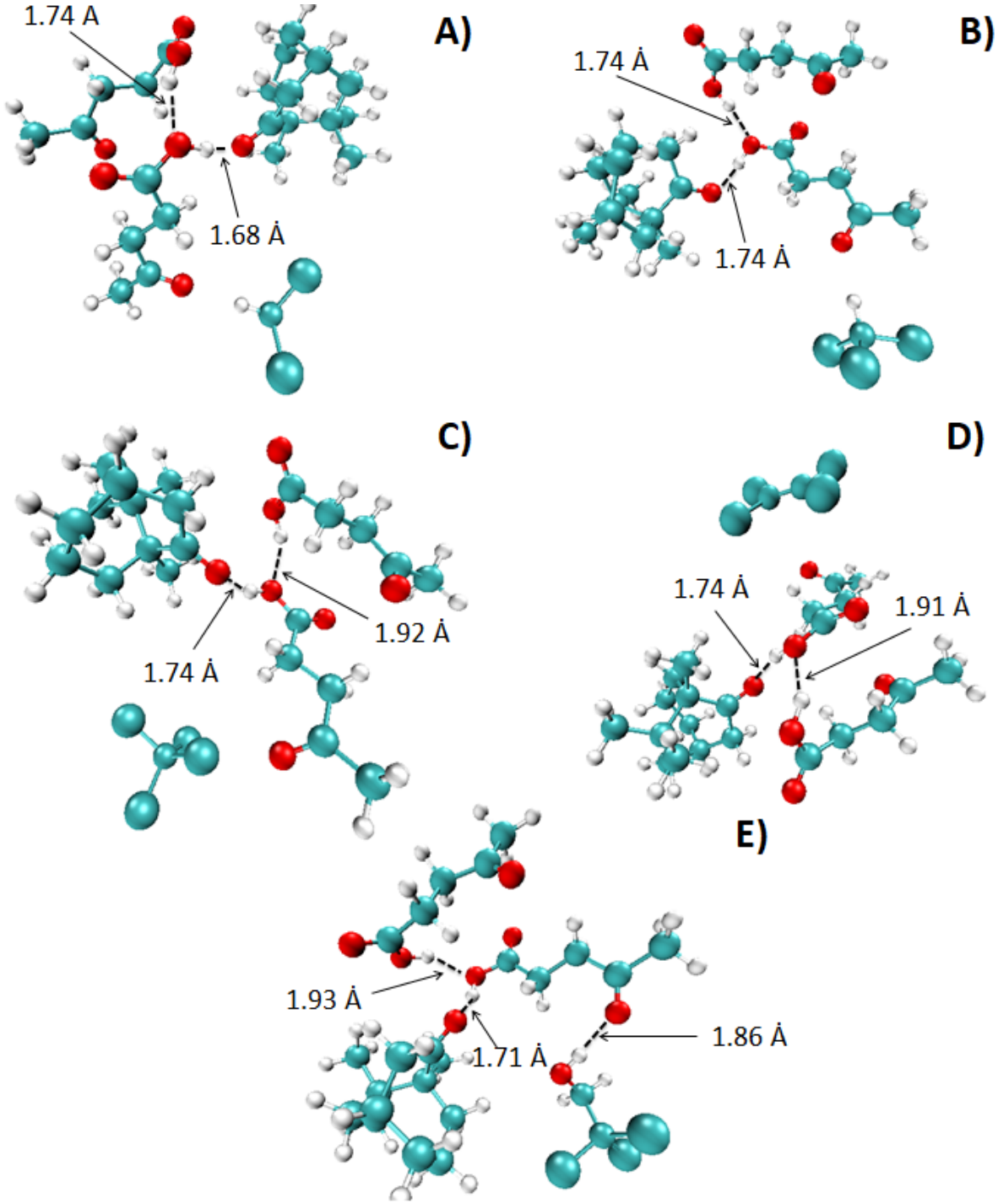

Figure S21 The structures of C:Lev (1:2) – VOX complexes after geometric optimization: A) C:Lev (1:2) – DCM; B) C:Lev (1:2)– CF; C) C:Lev (1:2) – TCM; D) C:Lev (1:2) – TCE; E) C:Lev (1:2) – TCEtOH.

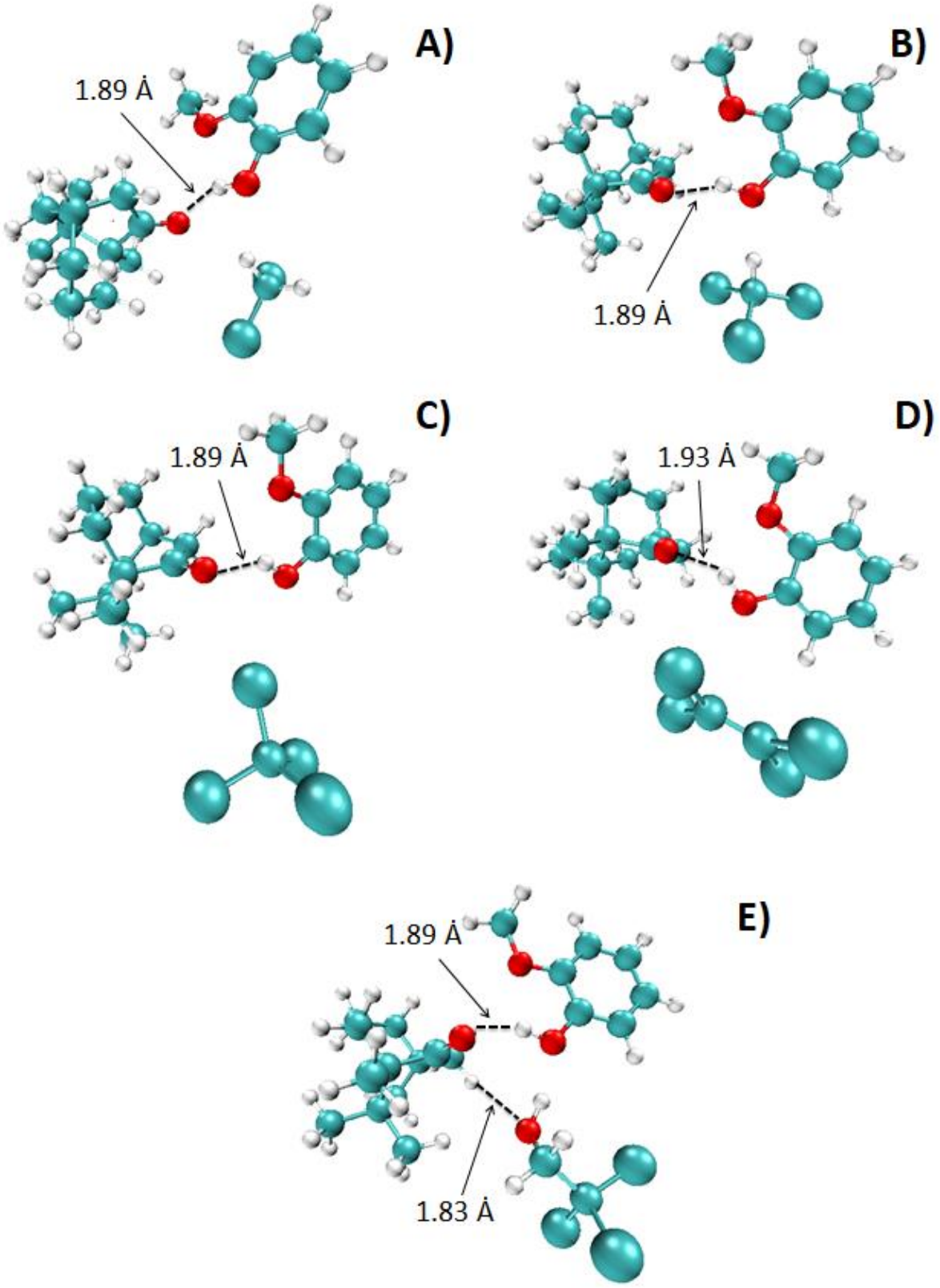

Figure S22 The structures of C:Gu (1:1) – VOX complexes after geometric optimization: A) C:Gu (1:1) – DCM; B C:Gu (1:1) - CF; C) C:Gu (1:1) – TCM; D) C:Gu (1:1) – TCE; E) C:Gu (1:1) – TCEtOH.

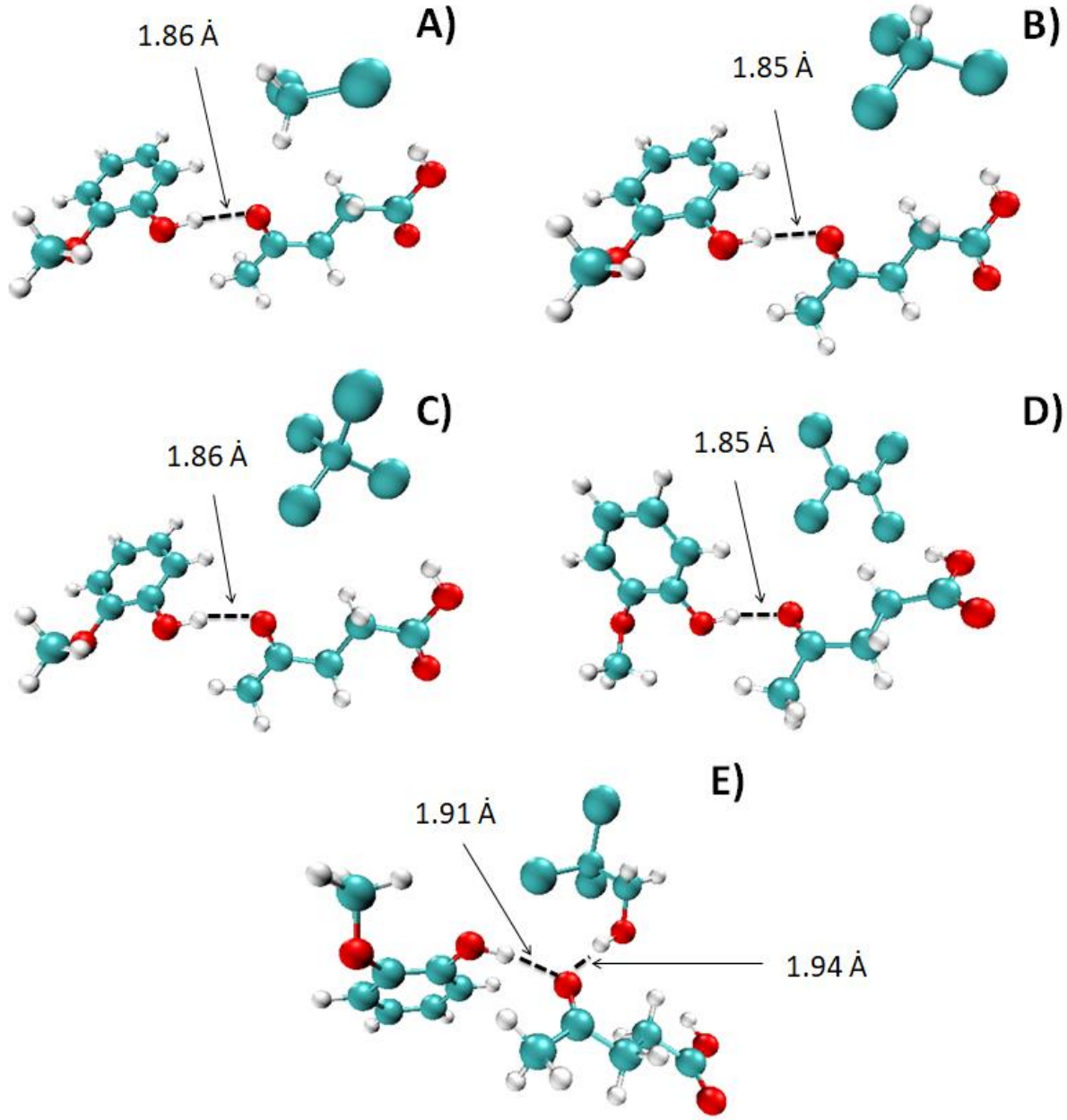

Figure S23 The structures of Gu:Lev (1:1) – VOX complexes after geometric optimization: A) Gu:Lev (1:1) – DCM; B Gu:Lev (1:1) - CF; C) Gu:Lev (1:1) – TCM; D) Gu:Lev (1:1) – TCE; E) Gu:Lev (1:1)– TCEtOH.

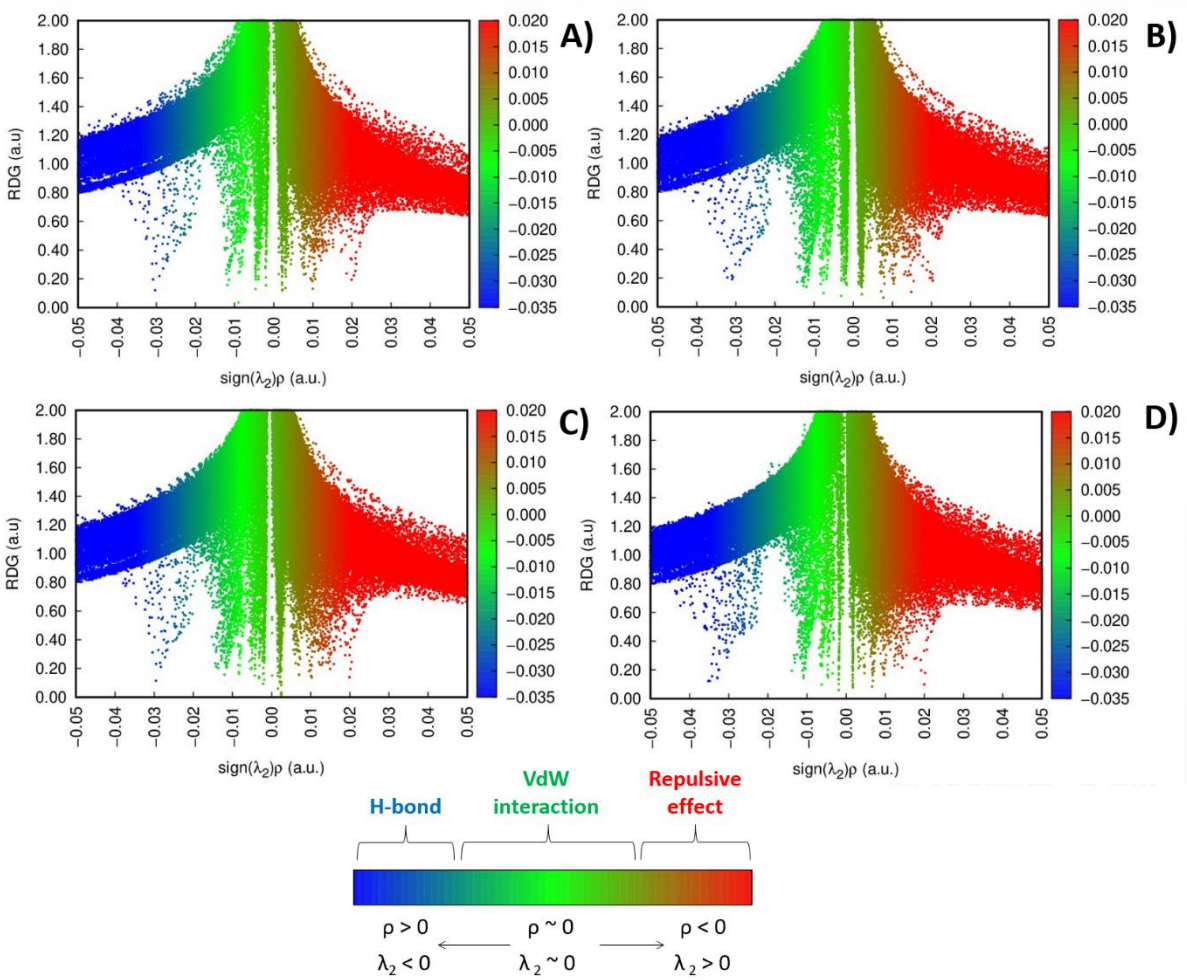

Figure S24 2D plots of RDG versus the electron density multiplied by the sign of the second Hessian eigenvalue for: ASyr:Lev (1:1) – CF; B) Syr:Lev (1:1) – TCM; C) Syr:Lev (1:1) – TCE; D) Syr:Lev (1:1) – TCEtOH. The red area represents repulsive effects; blue area - H-bonding; green area - van der Waals interactions.

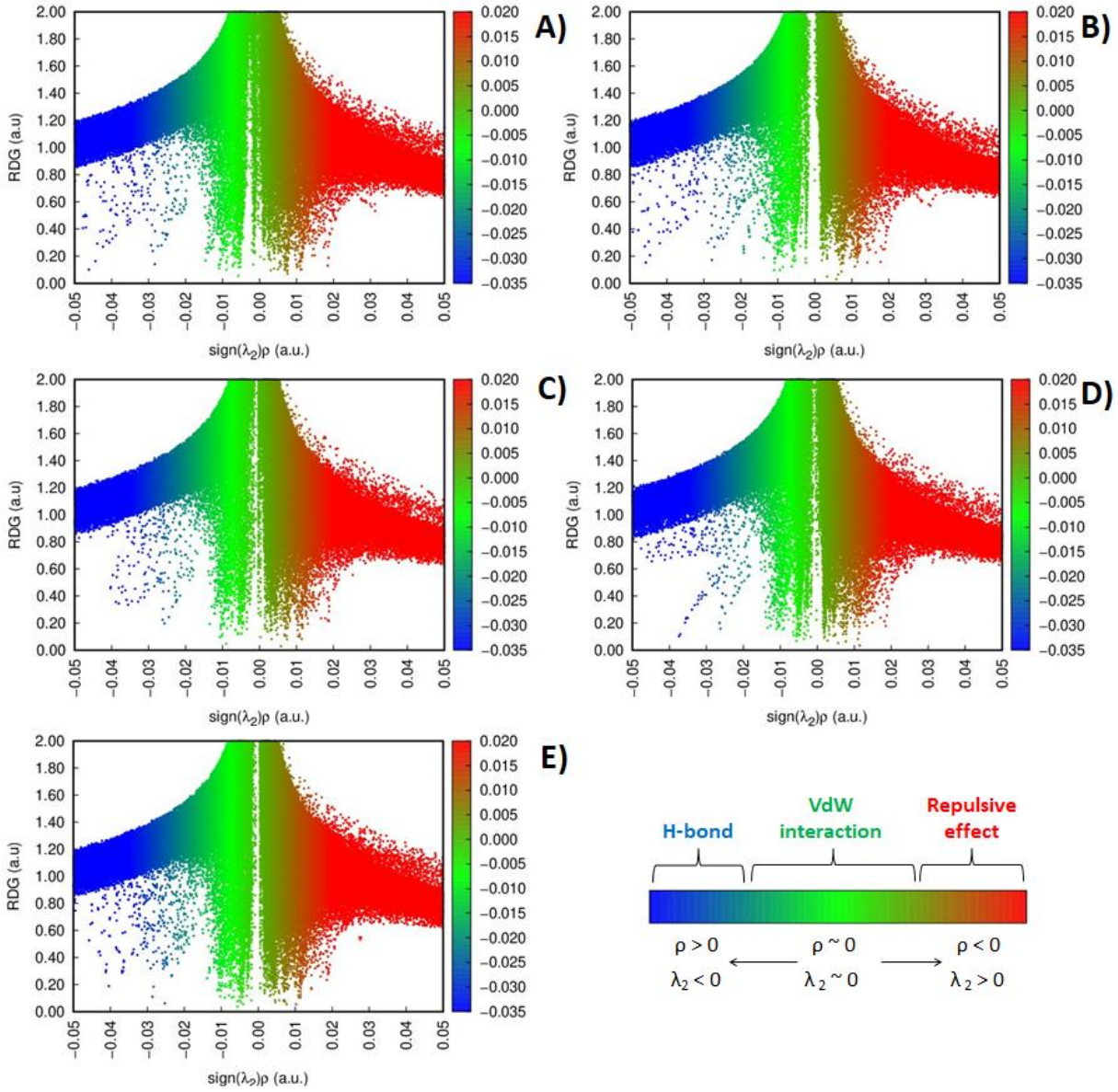

Figure S25 2D plots of RDG versus the electron density multiplied by the sign of the second Hessian eigenvalue for: A) C:Lev (1:2) – DCM; B) C:Lev (1:2)–CF; C) C:Lev (1:2)– TCM; D) C:Lev (1:2)– TCE; E) C:Lev (1:2)– TCEtOH. The red area represents repulsive effects; blue area - H-bonding; green area -van der Waals interactions.

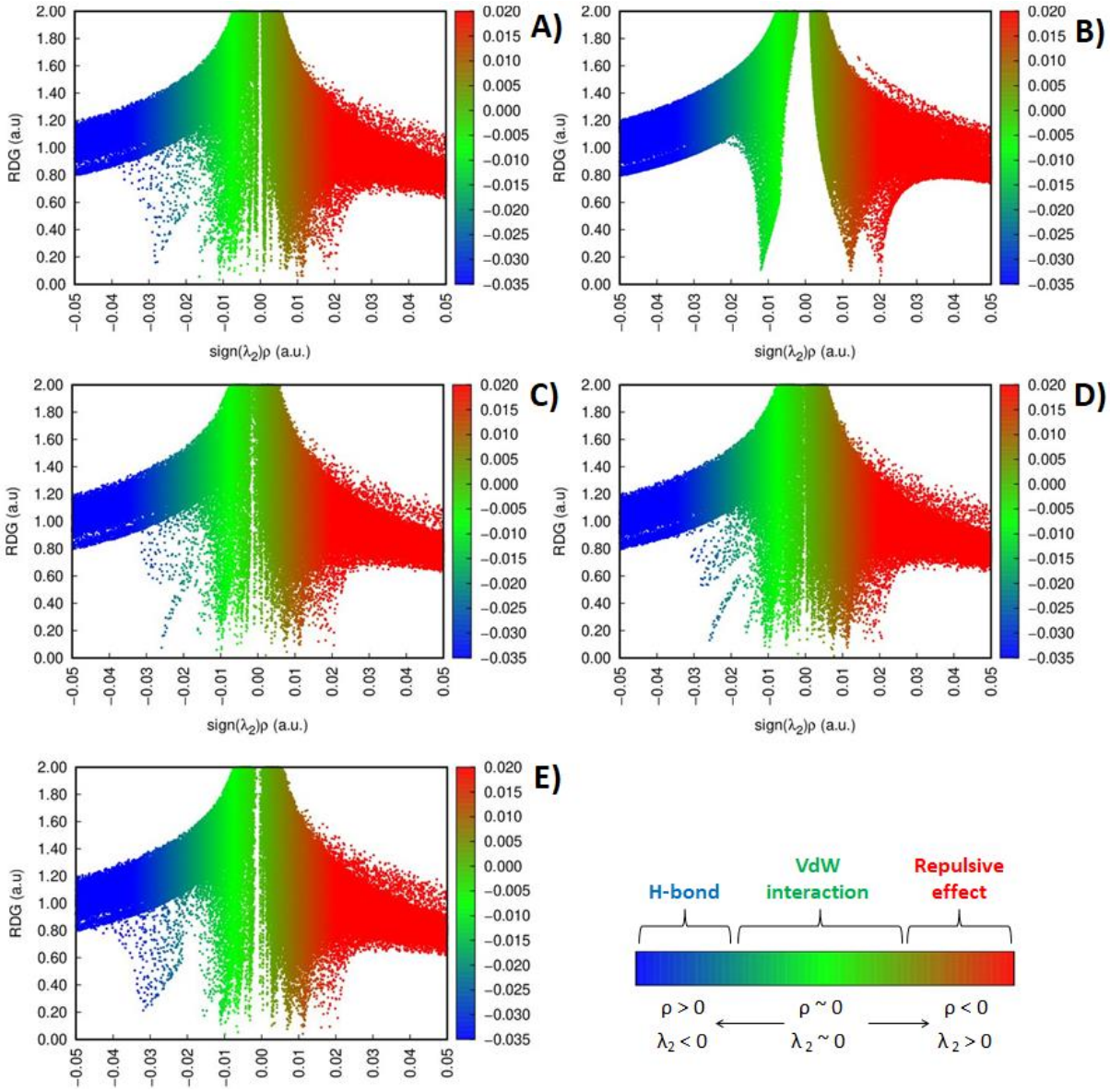

Figure S26 2D plots of RDG versus the electron density multiplied by the sign of the second Hessian eigenvalue for: A) C:Gu (1:1) – DCM; B) C:Gu (1:1) –CF; C) C:Gu (1:1) – TCM; D) C:Gu (1:1) – TCE; E) C:Gu (1:1) – TCEtOH. The red area represents repulsive effects; blue area - H-bonding; green area -van der Waals interactions.

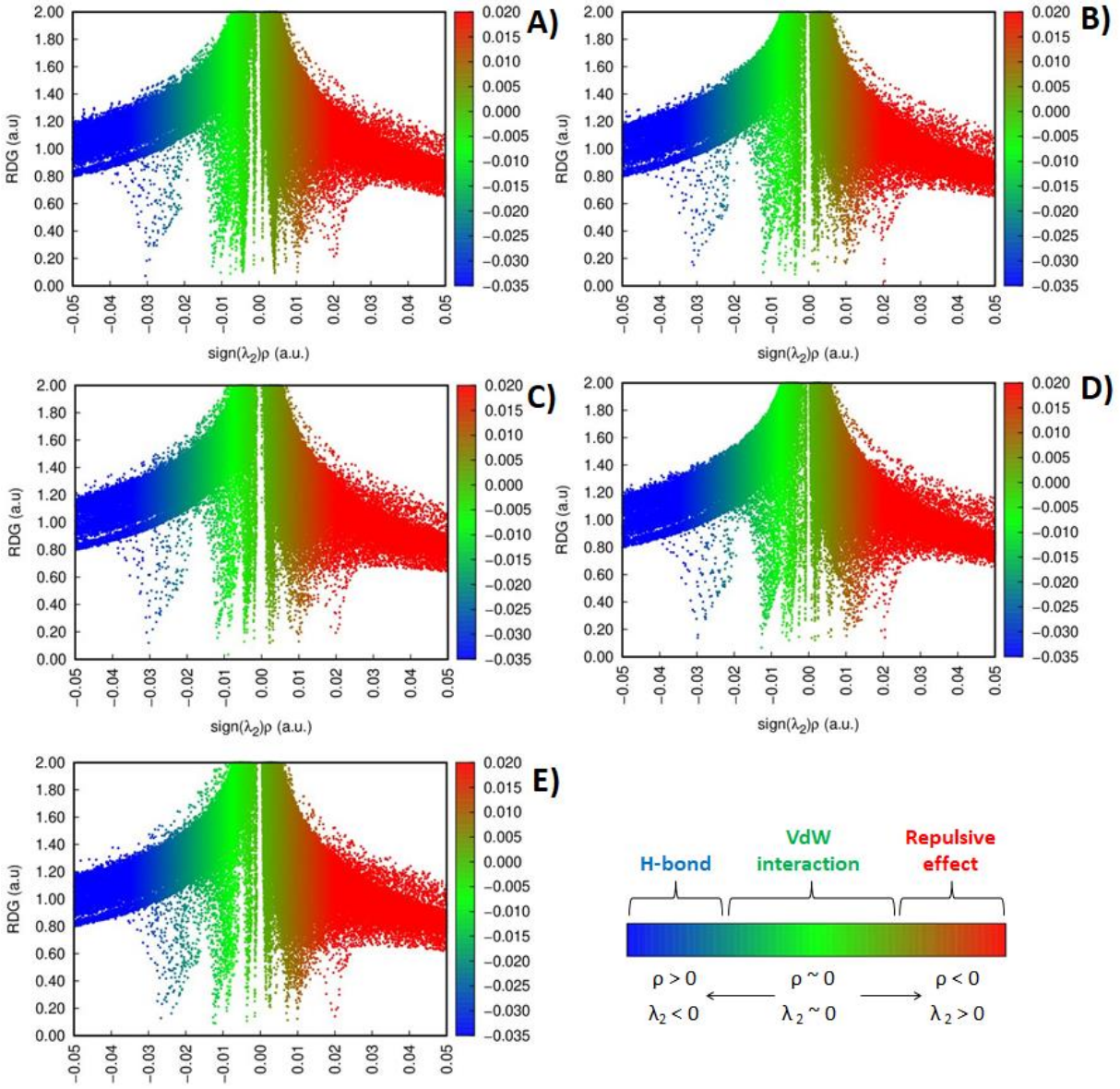

Figure S27 2D plots of RDG versus the electron density multiplied by the sign of the second Hessian eigenvalue for: A) G:Lev (1:1) – DCM; B) G:Lev (1:1) –CF; C) G:Lev (1:1) – TCM; D) G:Lev (1:1) – TCE; E) G:Lev (1:1) – TCEtOH. The red area represents repulsive effects; blue area - H-bonding; green area -van der Waals interactions.

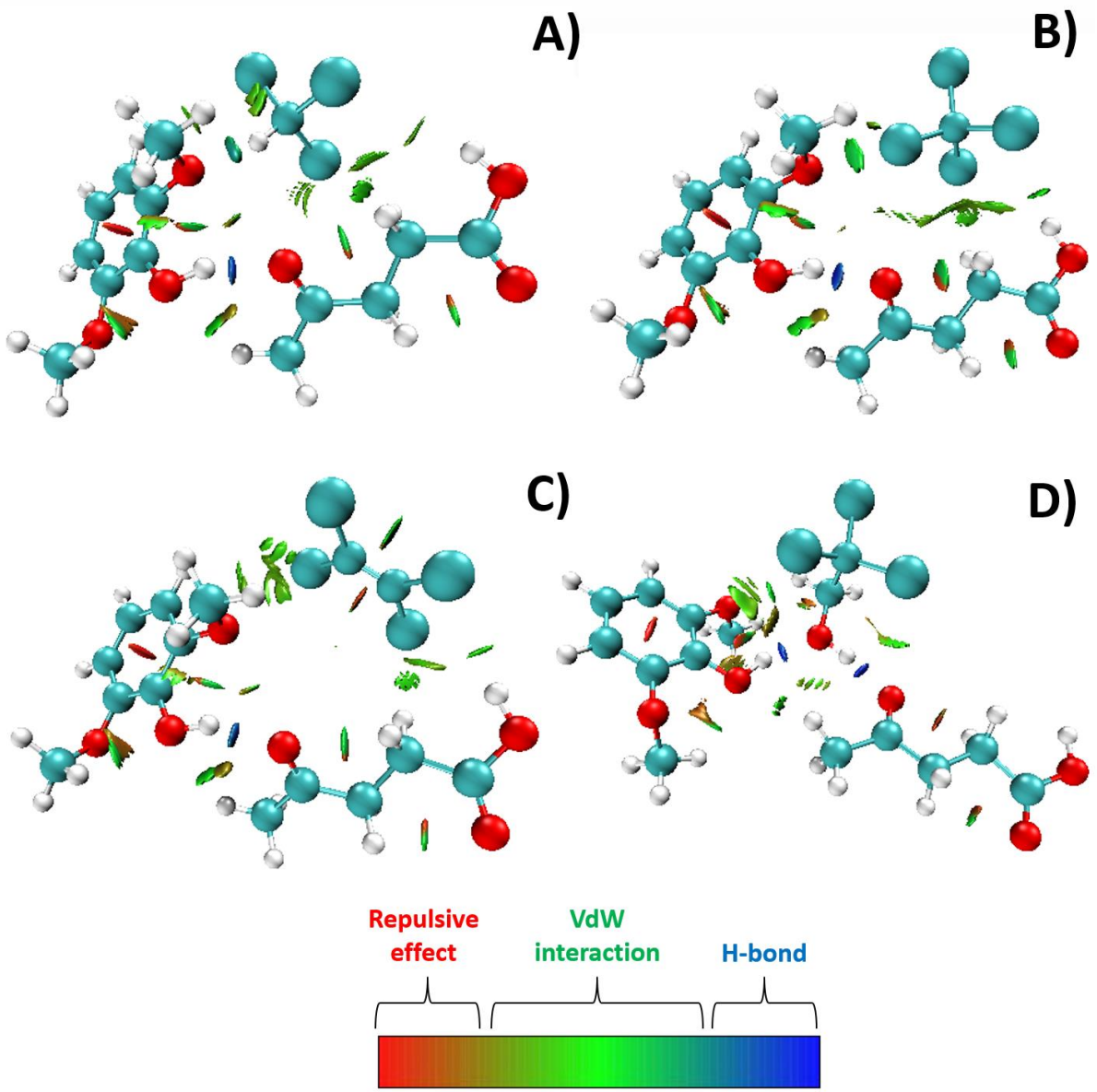

Figure S28 Reduced density gradient (RDG) isosurfaces (s=0.5 a.u.) of studied DES-VOX complexes: A) Syr:Lev (1:1) – CF; B) Syr:Lev (1:1) – TCM; C) Syr:Lev (1:1) – TCE; D) Syr:Lev (1:1) – TCEtOH. The red area represents repulsive effects; blue area - H-bonding; green area – van der Waals interactions.

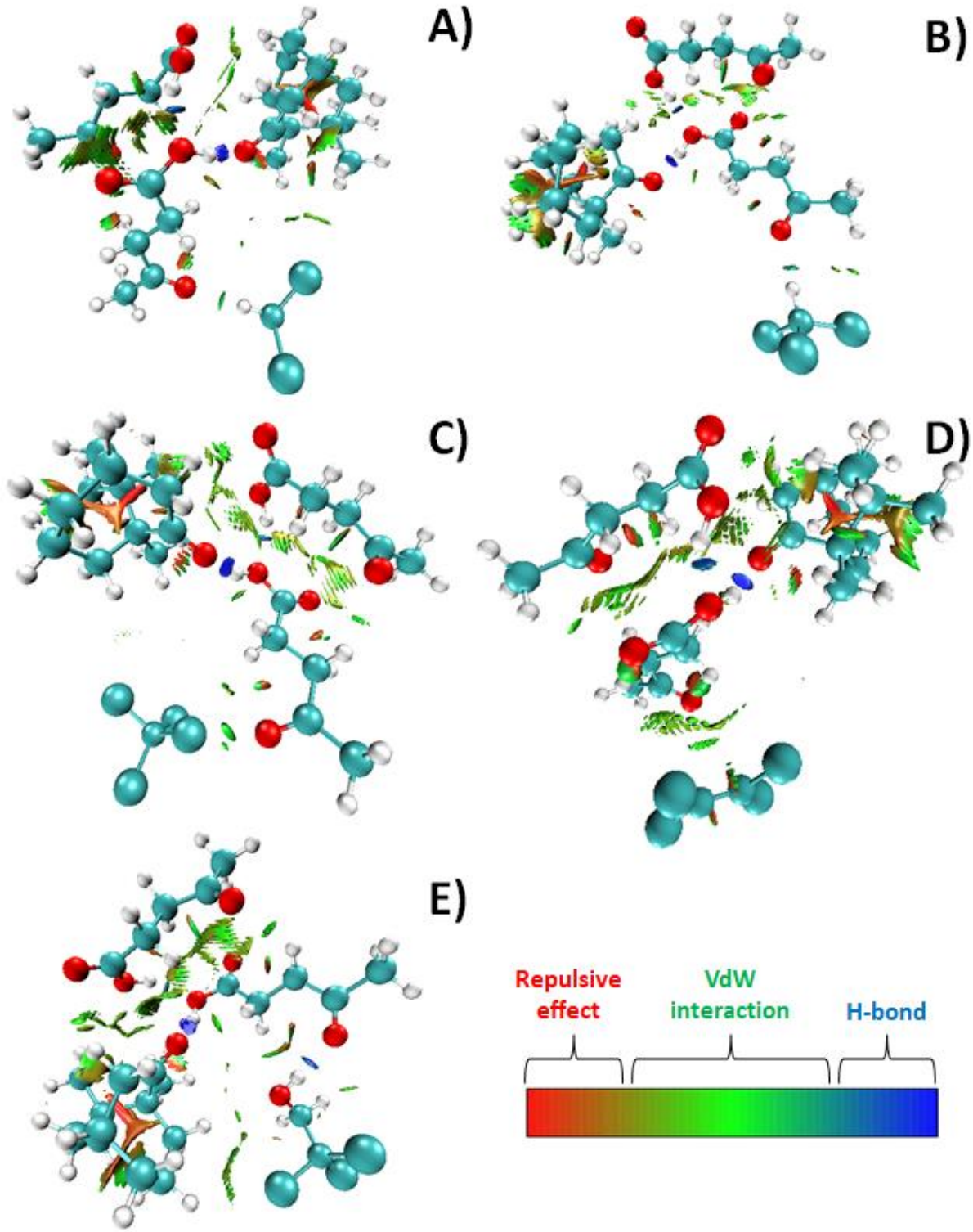

Figure S29 Reduced density gradient (RDG) isosurfaces (s=0.5 a.u.) of studied DES-VOX complexes: A) C:Lev (1:2) – DCM; B) C:Lev (1:2)–CF; C) C:Lev (1:2)– TCM; D) C:Lev (1:2)– TCE; E) C:Lev (1:2)– TCEtOH. The red area represents repulsive effects; blue area - H-bonding; green area -van der Waals interactions.

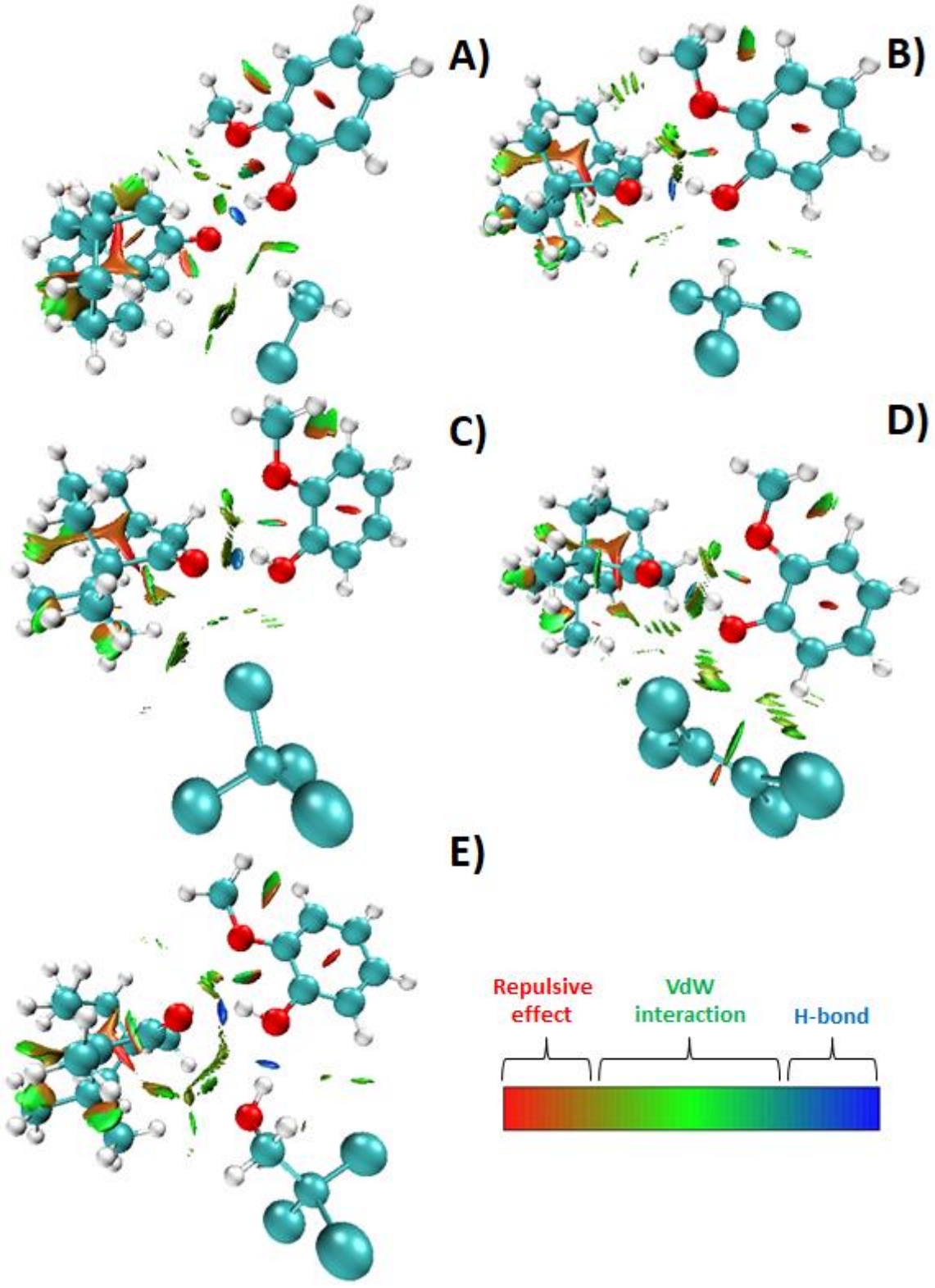

Figure S30 Reduced density gradient (RDG) isosurfaces (s=0.5 a.u.) of studied DES-VOX complexes: A) C:Gu (1:1) – DCM; B) C:Gu (1:1) –CF; C) C:Gu (1:1) – TCM; D) C:Gu (1:1) – TCE; E) C:Gu (1:1) – TCEtOH. The red area represents repulsive effects; blue area - H-bonding; green area -van der Waals interactions.

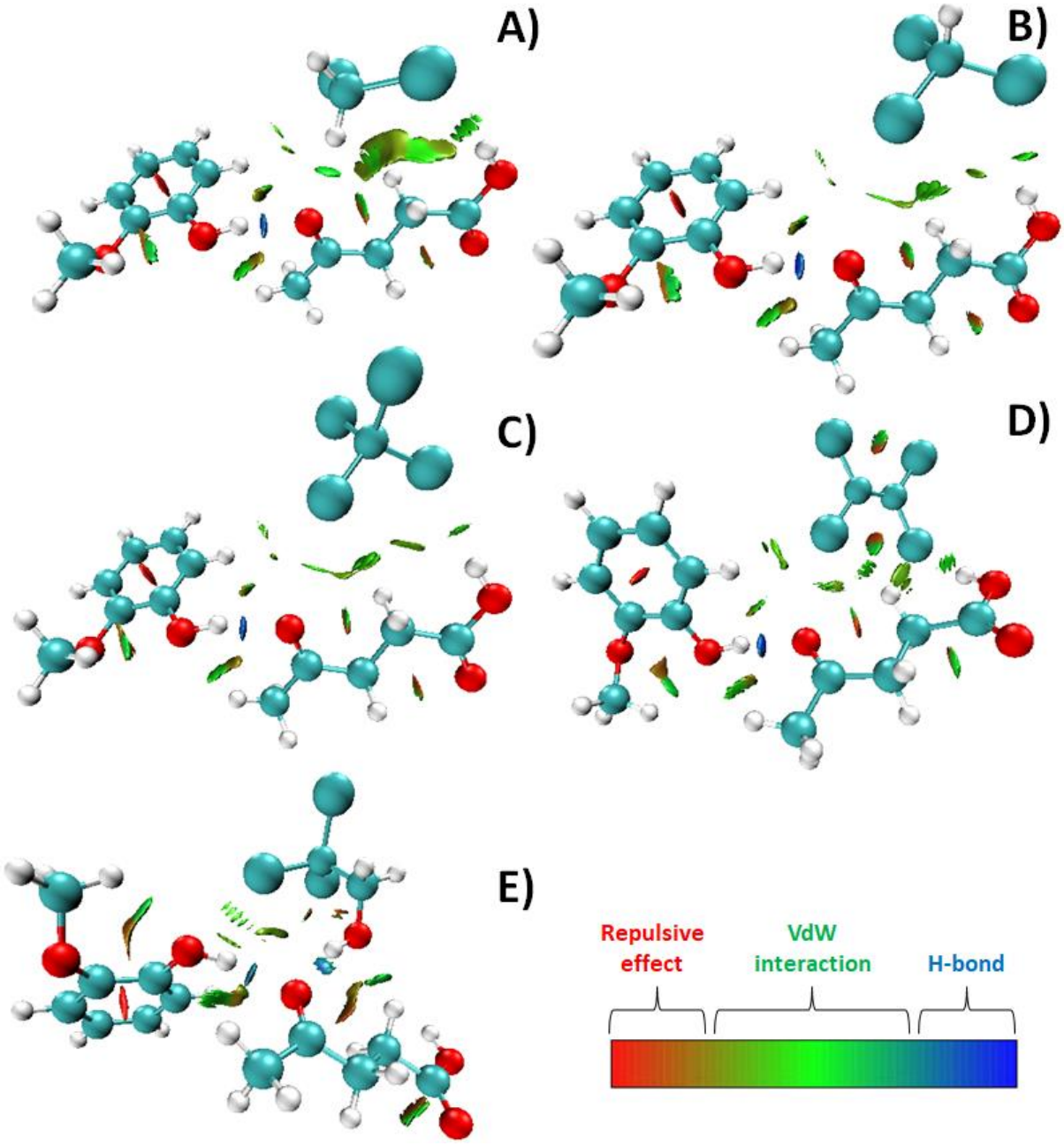

Figure S31 Reduced density gradient (RDG) isosurfaces (s=0.5 a.u.) of studied DES-VOX complexes: A) G:Lev (1:1) – DCM; B) G:Lev (1:1) –CF; C) G:Lev (1:1) – TCM; D) G:Lev (1:1) – TCE; E) G:Lev (1:1) – TCEtOH. The red area represents repulsive effects; blue area - H-bonding; green area -van der Waals interactions.

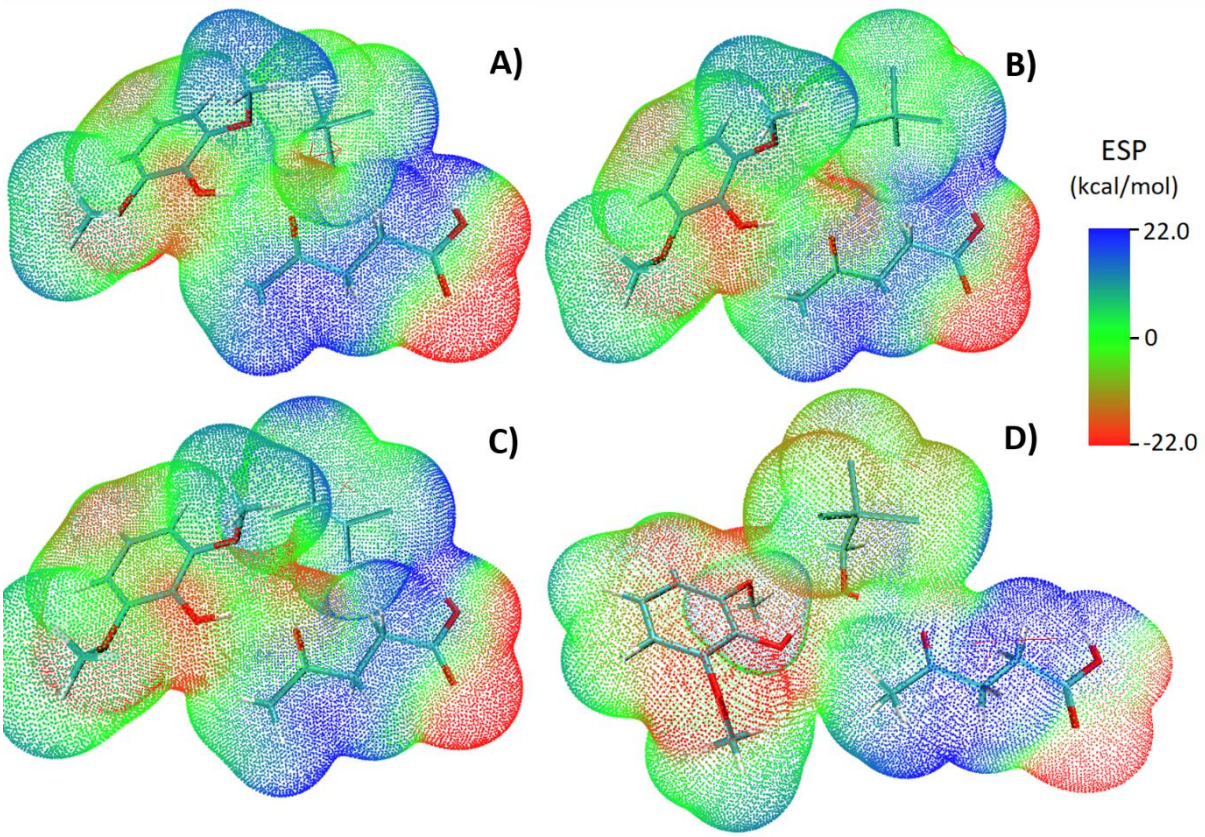

Figure S32 Electrostatic potential (ESP) mapped on electron total density with an isovalue 0.001 for: A) Syr:Lev (1:1) – CF; B) Syr:Lev (1:1) – TCM; C) Syr:Lev (1:1) – TCE; D) Syr:Lev (1:1) – TCEtOH. Blue area are positively charged; red regions are negatively charged; green are neutrally charged.

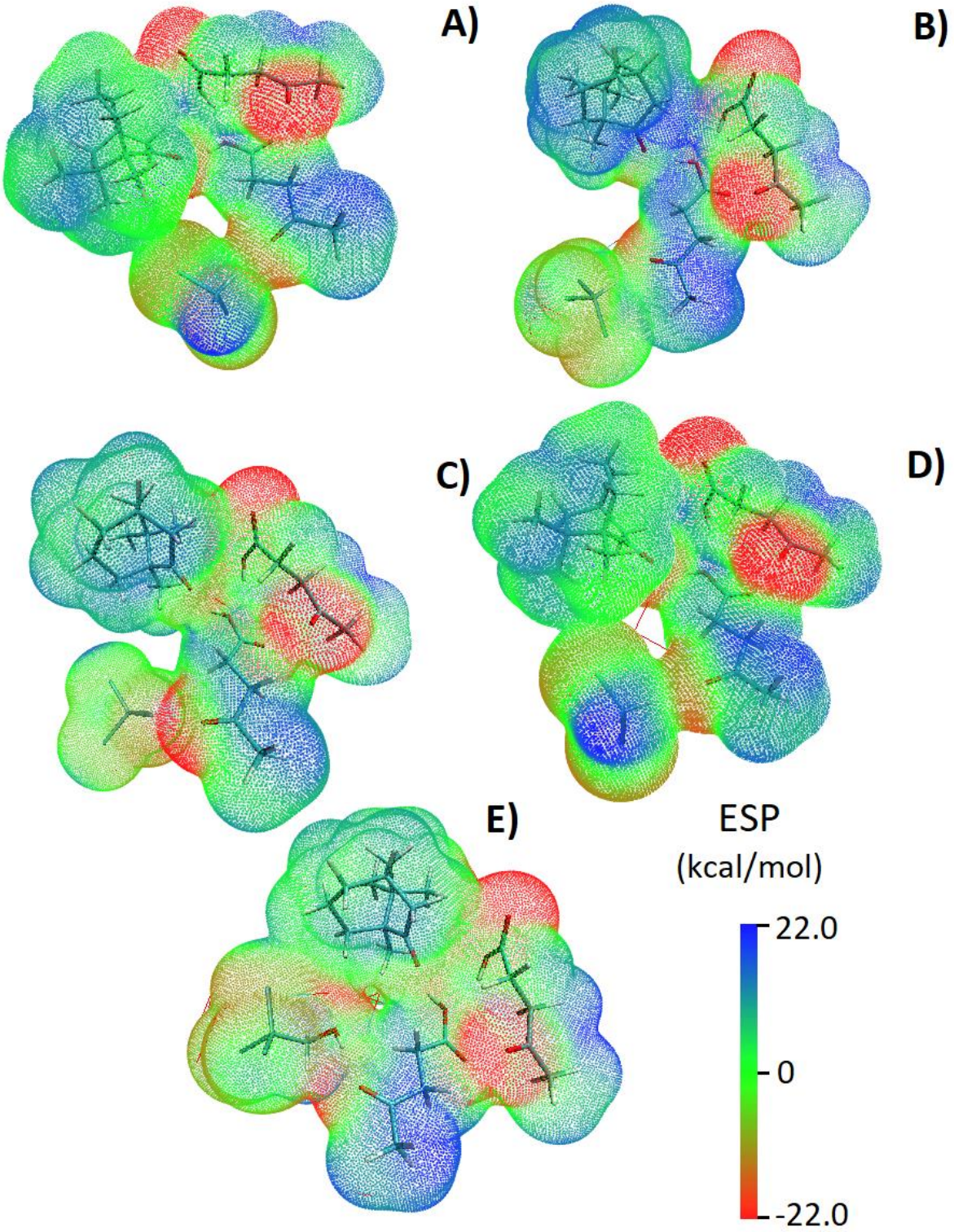

Figure S33 Electrostatic potential (ESP) mapped on electron total density with an isovalue 0.001 for: A) C:Lev (1:2) – DCM; B) C:Lev (1:2)–CF; C) C:Lev (1:2)– TCM; D) C:Lev (1:2)– TCE; E) C:Lev (1:2)– TCEtOH. Blue area are positively charged; red regions are negatively charged; green are neutrally charged.

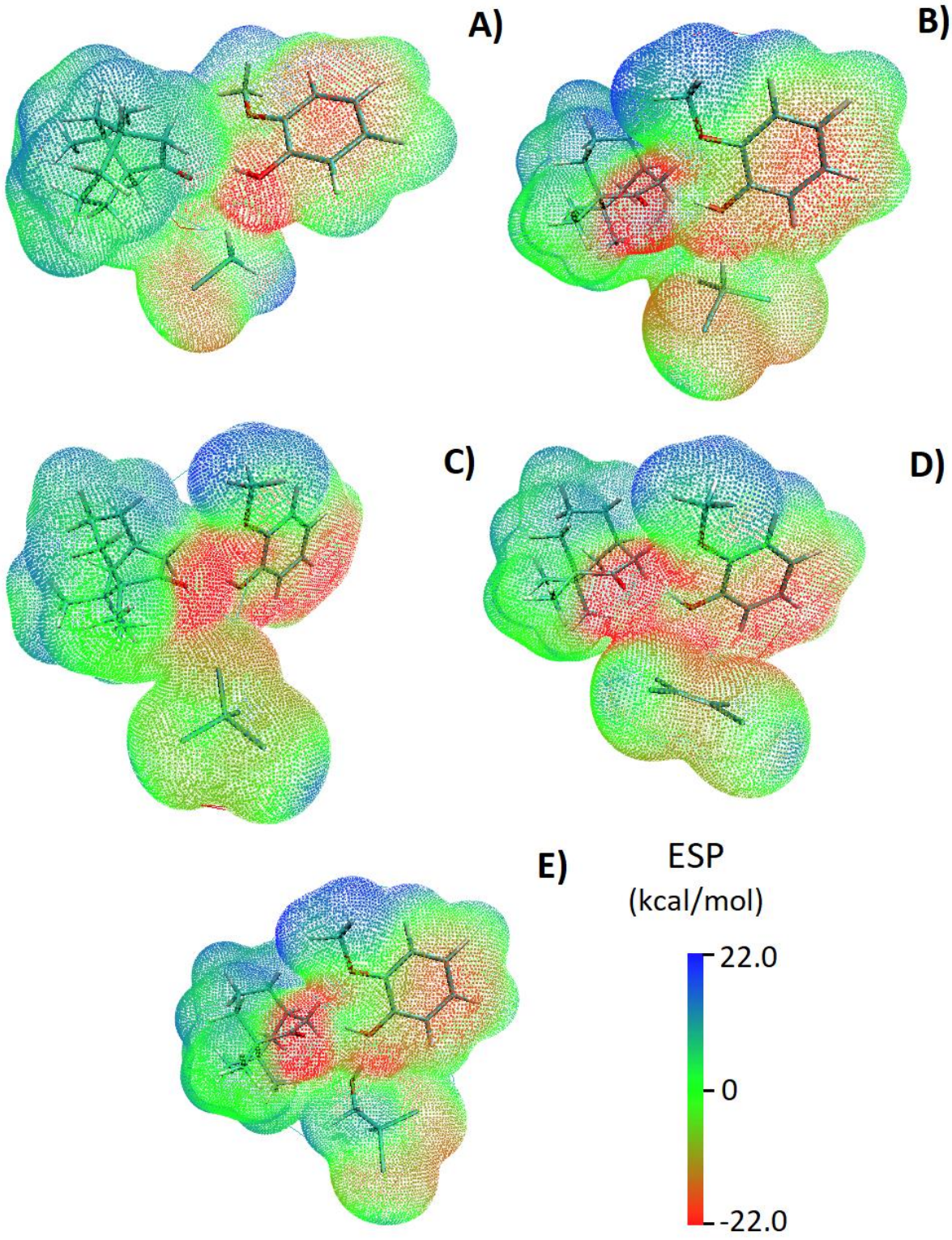

Figure S34 Electrostatic potential (ESP) mapped on electron total density with an isovalue 0.001 for: A) C:Gu (1:1) – DCM; B) C:Gu (1:1) - CF; C) C:Gu (1:1)– TCM; D) C:Gu (1:1)– TCE; E) C:Gu (1:1)– TCEtOH. Blue area are positively charged; red regions are negatively charged; green are neutrally charged.

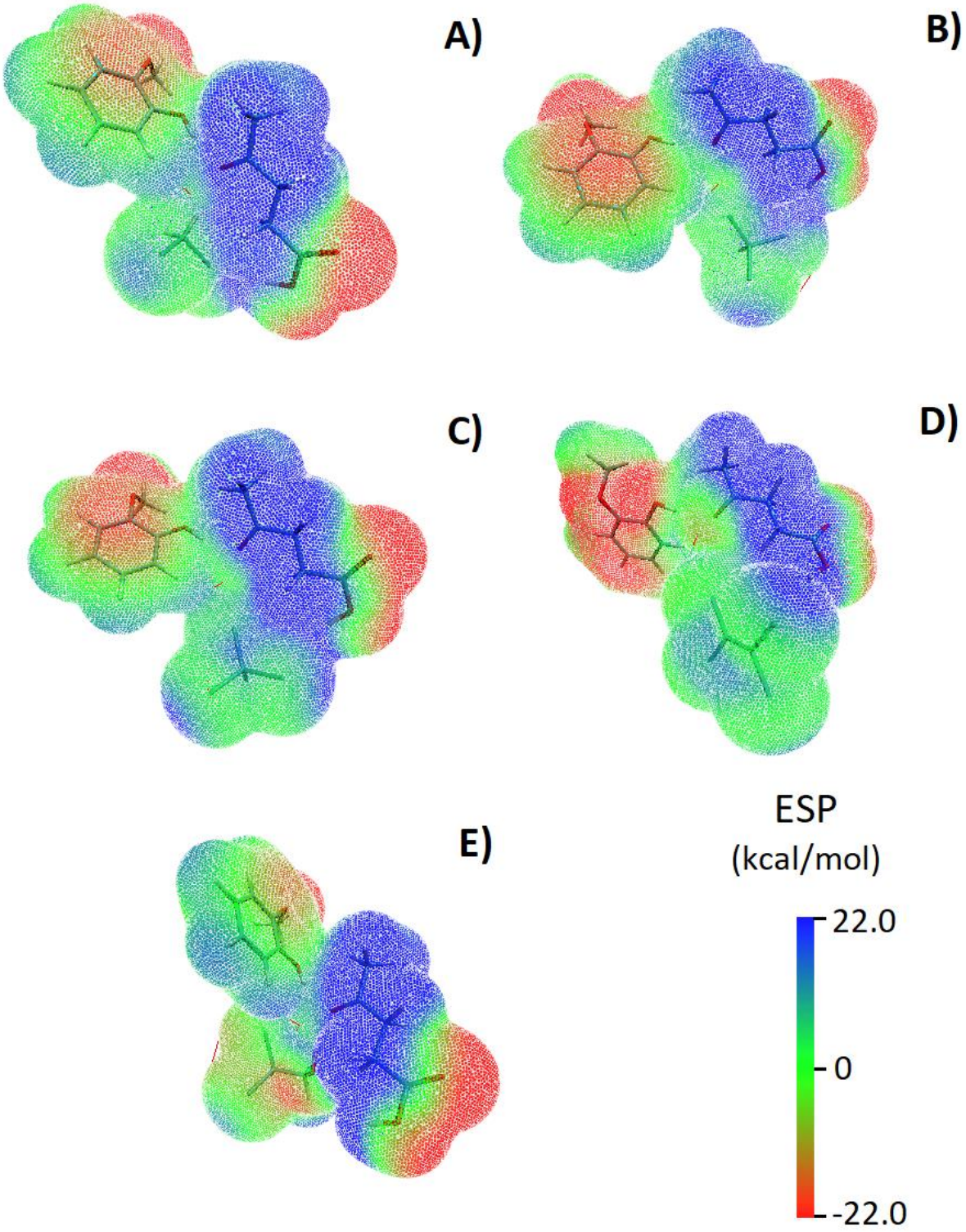

Figure S35 Electrostatic potential (ESP) mapped on electron total density with an isovalue 0.001 for: A) G:Lev (1:1) – DCM; B) G:Lev (1:1) –CF; C) G:Lev (1:1) – TCM; D) G:Lev (1:1) – TCE; E) G:Lev (1:1) – TCEtOH. Blue area are positively charged; red regions are negatively charged; green are neutrally charged.

Table S1 Comparison of the developed procedure of VOX absorption with other absorption or adsorption procedures.

Sorbent type	Type of VOX	Capacity [mg/g]	Gas type	Process conditions	Sorbent price per 1 kg	Ref.
ChCl:U (1:2)	DCM	0.2	air	Temperature: 30°C Flow rate: n.d. Pressure: n.d.	44.6 €	[1]
ChCl:EG (1:2)	DCM	0.26	air	Temperature: 30°C Flow rate: n.d. Pressure: n.d.	37.5 €	[1]
ChCl:Gly (1:2)	DCM	0.24	air	Temperature: 30°C Flow rate: n.d. Pressure: n.d.	40.1 €	[1]
ChCl:Lev (1:2)	DCM	0.27	air	Temperature: 30°C Flow rate: n.d. Pressure: n.d.	42.5 €	[1]
TBPB:Gly (1:1)	DCM	0.28	air	Temperature: 30°C Flow rate: n.d. Pressure: n.d.	199.9 €	[1]
TBPB:Lev (1:6)	DCM	0.29	air	Temperature: 30°C Flow rate: n.d. Pressure: n.d.	76.1 €	[1]
TBAB:DA (1:2)	DCM	0.3	air	Temperature: 30°C Flow rate: n.d. Pressure: n.d.	320.5 €	[1]
UiO-66	DCM	510.3	air	Temperature: 25°C Pressure: 44 kPa	79207.20 €	[2]
activated carbon	CF DCM CM	213.4 123.9 22.2	N_2	Temperature: 35°C Flow rate: 100 mL/min Pressure: 1.5 atm	12.16 €	[3]
ZIF-8/graphene oxide	DCM	240.0	air	Temperature: 25°C Flow rate: 20 ml/min.	7689.0 €	[4]
[Bmim][NTf2]	DCM	100	air	Temperature: 30°C Flow rate: n.d. Pressure: 10 kPa	950 €	[5]
[Bmim][PF6]	DCM	110	air	Temperature: 30°C Flow rate: n.d. Pressure: 10 kPa	2450.8 €	[5]
[Bmim][BF4]	DCM	130	air	Temperature: 30°C Flow rate: n.d. Pressure: 10 kPa	750 €	[5]
[Bmim][DCA]	DCM	140	air	Temperature: 30°C Flow rate: n.d. Pressure: 10 kPa	2494.5 €	[5]
[Bmim][SCN]	DCM	150	air	Temperature: 30°C Flow rate: n.d. Pressure: 10 kPa	892.8 €	[5]
[Emim][SCN]	DCM	120	air	Temperature: 30°C Flow rate: n.d. Pressure: 10 kPa	4934	[5]
Gu:C:Lev (1:1:3)	DCM	55	N_2	Temperature: 25°C Flow rate: 50 mL/min Pressure: 10 kPa	29.0 €	[6]
Syr:Lev (1:1)	DCM CF TCM TCE TCEtOH	304 420 360 292 661	Biogas (58% CH_4, 38 CO_2, 2% H_2O, 2% N_2)	Temperature: 25°C Flow rate: 50 mL/min Pressure: 10 kPa	263.5 €	This studies
C:Gu (1:1)	DCM CF TCM	215 561.5 320	Biogas (58% CH_4, 38 CO_2, 2% H_2O, 2% N_2)	Temperature: 25°C Flow rate: 50 mL/min Pressure: 10 kPa	32.78 €	This studies

	TCE	262.4				
	TCEtOH	275.3				
C:Lev (1:2)	DCM	181	Biogas (58%	Temperature: 25°C	24.02 €	This studies
	CF	401.5	CH_4, 38 CO_2, 2%	Flow rate: 50 mL/min		
	TCM	143.5	H_2O, 2% N_2)	Pressure: 10 kPa		
	TCE	248				
	TCEtOH	198.15				
Gu:Lev (1:1)	DCM	130.7	Biogas (58%	Temperature: 25°C	36.01 €	This studies
	CF	399.5	CH_4, 38 CO_2, 2%	Flow rate: 50 mL/min		
	TCM	115.8	H_2O, 2% N_2)	Pressure: 10 kPa		
	TCE	154				
	TCEtOH	161.2				

[Bmim][NTf2] *- 1-Butyl-3-methylimidazolium bis(trifluoromethylsulfonyl)imide;* ***[Bmim][PF6]*** *- 1-Butyl-3-methylimidazolium hexafluorophosphate;* ***[Bmim][BF4]*** *- 1-Butyl-3-methylimidazolium tetrafluoroborate;* ***[Bmim][DCA]*** *- 1-Butyl-3-methylimidazolium dicyanamide;* ***[Bmim][SCN]*** *- 1-Butyl-3-methylimidazolium thiocyanate;* ***[Emim][SCN]*** *- 1-Ethyl-3-methyl-imidazolium-thiocyanate;* ***ChCl*** *– choline chloride;* ***CM****- Chloromethane;* ***DA*** *– decanoic acid;* ***EG*** *– ethylene glycol;* ***Gly*** *– glycerol;* ***U*** *– urea;* ***UiO-66*** *- (Universitetet i Oslo) a metal organic framework;* ***TBAB*** *– tetrabutylammonium bromide;* ***TBPB*** *- tetrabutylphosphonium bromide*

References

[1] L. Moura, T. Moufawad, M. Ferreira, H. Bricout, S. Tilloy, E. Monflier, M. F. Costa Gomes, D. Landy, S. Fourmentin, *Environ. Chem. Lett.* **2017**, *15*, 747–753.

[2] L. Zhou, X. Zhang, Y. Chen, *Mater. Lett.* **2017**, *197*, 167–170.

[3] J. Lemus, M. Martin-Martinez, J. Palomar, L. Gomez-Sainero, M. A. Gilarranz, J. J. Rodriguez, *Chem. Eng. J.* **2012**, *211–212*, 246–254.

[4] Y. Zhou, L. Zhou, X. Zhang, Y. Chen, *Microporous Mesoporous Mater.* **2016**, *225*, 488–493.

[5] W. Wu, T. Li, H. Gao, D. Shang, W. Tu, B. Wang, X. Zhang, *Guocheng Gongcheng Xuebao/The Chinese J. Process Eng.* **2019**, *19*, 173–180.

[6] E. Słupek, P. Makoś, J.Gębicki, *Arch. Environ. Prot.* **2020**, *46*, 41–46.